Design and experimental validation of an adaptive fast-finite-time observer on uncertain electro-hydraulic systems

Published Version:
Razmjooei H., Palli G., Abdi E., Terzo M., Strano S. (2023). Design and experimental validation of an adaptive fast-finite-time observer on uncertain electro-hydraulic systems. CONTROL ENGINEERING PRACTICE, 131(February 2023), 1-17 [10.1016/j.conengprac.2022.105391].

Availability:
This version is available at: https://hdl.handle.net/11585/912988 since: 2023-11-24

Published:
DOI: http://doi.org/10.1016/j.conengprac.2022.105391

Design and Experimental Validation of an Adaptive Fast-Finite-Time Observer on Uncertain Electro-Hydraulic Systems

Hamid Razmjooei [a], **Gianluca Palli** [a], **Elahe Abdi** [b], **Mario Terzo** [c], and **Salvatore Strano** [c]

[a] Department of Electrical, Electronic, and Information Engineering, University of Bologna, Bologna, Italy (Emails: hamid.razmjooei@unibo.it and gianluca.palli@unibo.it)

[b] Department of Mechanical and Aerospace Engineering, Monash University, Melbourne, Australia (elahe.abdi@monash.edu)

[c] Department of Industrial Engineering, University of Naples Federico II, Naples, Italy (Emails: salvatore.strano@unina.it, mario.terzo@unina.it)

Abstract

This paper presents the design of an adaptive fast-finite-time extended state observer for electro-hydraulic actuator systems. First, the system model is divided into three parts, and fast-finite-time state observers are designed independently for each part, which guarantee the fast-finite-time uniformly ultimate boundedness of the estimation errors. Then, based on the designed state observers and without neither any knowledge about the upper bounds of the uncertainties nor its derivative, supplementary observers are presented to estimate the unknown terms. Rigorous analyses of the proposed strategy are provided through the Lyapunov approach. The suggested adaptive framework can improve the convergence rate for zones both far from the equilibrium points and around them, where the adaptive gains are computed based on the evaluation of the absolute value of the observation errors, achieving finite-time estimate of both the full state variables as well as uncertainties. Comparative simulations are presented to analyze the effectiveness of the proposed observers. Finally, the effectiveness of the proposed approach in real-life conditions is demonstrated through experimental studies.

Key words: Adaptive fast-finite-time extended state observer, Electro-hydraulic actuator systems, Nonlinear observer, Uniformly ultimately boundness.

1. Introduction

Electro-Hydraulic Actuator (EHA) systems, which provide a high power-to-weight ratio, high stiffness, and high load efficiency, have been widely used in mechatronic systems [1, 2]. The EHA systems include nonlinearities and several uncertainties including unmodeled dynamics, disturbances, and frictions with dynamics that are not exactly known and limiting their broad applicability [3]. Due to these challenges, there have been restrictions in the accomplishment of exact modeling. Different techniques have been employed to model nonlinearities and uncertainties, where a simple solution is to equip the system with various sensors. In practice, some difficulties such as space limitations and measurement noise occur, thus measuring the full system states is not simple and often not possible. In this regard, an alternative approach is to equip only the main outputs of the system with sensors and design an observation algorithm to process the incomplete information collected by the sensors and construct a reliable estimation of all state variables [4]. Since estimating the state variables has been an essential process in achieving an acceptable dynamic performance in the EHA systems, therefore observers are a common option to reduce the number of sensors [5]. In recent years, several observation approaches have been presented that provide a reliable estimation of all state variables over an infinite time interval. However, in order to achieve safety and high steady-state precision performance, finite-time estimation is more important and strategic than asymptotic or exponential performance [6]. It is worth noting that, in the presence of uncertainties, external disturbances, and friction, exact estimation of state variables is not possible, therefore the ultimate boundedness concept is considered [7]. Within finite-time observers' context with the ultimate boundedness convergence, some strategies have been presented in the last few years.

In recent years, the Sliding Mode Observer (SMO) approach has been developed with widespread applications [8-11], where their performance is investigated through simulation and experimental studies, considering different sets of measurement noises, parametric uncertainties, and model nonlinearities. However, the standard version of the SMO is affected by some restrictions, leading to the potentially destructive chattering phenomenon in their convergence to a small neighborhood of zero [11]. To mitigate this drawback, the High-order Sliding Mode Observer (HO-SMO) has been introduced to reduce the chattering and the Terminal Sliding Mode Observer (TSMO) with finite-time convergence properties have alternatively been developed [12-15]. For instances, the performance of the HO-SMO has been analyzed compared with SMO and Kalman filter method, where its high efficiency to estimate the uncertainties was presented in [12]. However, a problem of these observers still remains, since if the initial conditions tend far from the equilibrium point, the convergence time grows unboundedly. Hence, it is more desirable for an observer to guarantee that the convergence is achieved in a short time interval regardless of the initial conditions. In this regard, fast finite-time observers using the concept of bi-limit homogeneity were first introduced in [16] and then studied in [17-20]. The fast finite-time approach is more powerful than the finite-time approach as it guarantees the boundedness of the convergence time almost independently from initial conditions. However, in addition to structural limitations, the gains of these observers are not easily computable. The fast finite-time observer presented in [20] is recognized as one of the leading strategies to estimate the full states of systems, as well as the uncertainties. However, the design of the observer gains with a straightforward framework is still an open problem.

In recent years, high gain extended state observers (HG-ESO) with straightforward framework have been investigated [21-23] to estimate the full states and external disturbances. From the studies reported in [21, 22], it is possible to conclude that HG-ESOs presents better performance for EHA systems under parametric uncertainties and model nonlinearities. The HG-ESO in [21, 22] is analyzed using simulated and experimental tests compared with conventional observers, demonstrating estimation of full state variables and total disturbances. Furthermore, time-varying observers with an exponential convergence were presented in [24-29]. Especially, [27] including some shortcomings, such as (1) Valid response only in a finite time interval, while in many applications it is important to have a valid response for a longer duration; (2) Unconsidered internal dynamics, while internal dynamics should be explicitly considered in the proof as it can act as an uncertainty in the values of the state variables; (3) Required prior knowledge of the uncertainties, while it is not often possible to measure them in practice. To overcome these restrictions, a time-varying gains observer has been presented due to its straightforward design and better robustness against uncertainties and internal dynamics [28, 29]. Although the authors have several publications in this field, the approach proposed in this paper is completely novel, with very limited overlap with previous publications. This paper is a combination of adaptive and fast finite-time frameworks that can improve the convergent rate for zones both far from the equilibrium points and around them, while references [6], [28], and [29] already presented a time-varying high-gain extended state observer under a different framework. In this paper, the adaptive gains are changed based on the evaluation of the absolute value of the observation errors, while the gains in the referred papers are changed over time without any adaptive criterion. On the other hand, although the previous approaches are valid schemes for observer design to simultaneously estimate state variables, uncertainties, and external disturbances, it is only applicable in single-input single-output canonical systems and they presents singularity problems, where its time-varying transformation grows unboundedly. Consequently, the time-varying approach proposed in this paper has potential for further progress.

It is worth noting that, although so far, some leading strategies has been highlighted and discussed for uncertain real-world systems, according to their shortcomings this subject has still remained an open problem for further improvement in EHA systems. Motivated by the above discussions, the problem of designing an adaptive fast-finite-time extended state observer (adaptive fast FT-ESO and/or AFFTESO) for EHA systems is addressed in this paper without neither any knowledge about the upper bounds of the uncertainties nor its derivative. The proposed AFFTESO can reconstruct the unmeasured state variables, external disturbances, and uncertainties in a finite time. In contrast to the earlier finite-time approaches, which only have a faster convergence rate around the equilibrium points, the proposed adaptive framework can improve the convergent rate for zones far from the equilibrium points. The gains of the proposed AFFTESO are changed based on the evaluation of the absolute value of the observation errors. Moreover, this adaptive strategy forces the proposed observer to estimate the output measured variables of the EHA system in a finite time, including simultaneous estimation of the external disturbances, friction force, dead-zone effects, and spool bias. First, the EHA model is divided into three parts and the fast finite-time state observers are presented for each part independently, guaranteeing fast-finite-time uniformly ultimate boundness (FFTUUB) of the estimation errors. Then, based on these designed state observers, supplementary similar observers are presented to estimate the unknown terms, where rigorous analyses of the proposed strategy are provided through the Lyapunov approach. Comparative simulations are presented to analyze the effectiveness of the proposed observers with respect to some leading literature approaches. According to the simulation results, it is possible to classify the different observer strategies according to the following list (in descending order of efficiency): AFFTESO, HG-ESO, HO-SMO, time-varying FT-ESO, and third-order FFTESO. Then, under adaptive and fixed gains, the proposed adaptive observer guarantees that the state estimation errors are uniformly bounded and the estimation error can approach an arbitrarily small value by choosing some design parameters appropriately. Finally, the effectiveness of the proposed approach in real-life conditions is demonstrated through experimental studies. Compared with the existing literature approaches, the main contributions of this paper are, 1) An AFFTESO is designed such that, without neither any knowledge about the upper bound of uncertainties nor its derivative, it is possible to estimate the full state of the nonlinear system as well as the uncertainties, achieving convergence of the observation error to a neighborhood of zero. 2) Adaptive gains are computed based on evaluation of the absolute value of the observation errors. 3) The proposed AFFTESO has a faster convergence rate for zones both far from the equilibrium points and around them.

It is worth noting that, the gain selection process has always been a concern and challenge in observer design. Although the adaptive gains in this paper are computed based on a evaluation of the absolute value of the observation errors, this selection does not follow an optimal procedure. In this regard, future activities will be devoted to presenting an optimal algorithm for the selection of all the observer parameters. The remainder of the paper is structured as follows. In Section 2, a fifth-order model of the EHA is illustrated and relevant definitions and conditions for FFTUUB are presented. In Section 3, the AFFTESOs are designed. In Sections 4 simulation and experimental results demonstrate the effectiveness of the AFFTESOs. Finally, conclusions and future plans are presented in Section 5.

2. Preliminaries and system descriptions

Figure 1 shows a schematic representation and experimental setup used to test the proposed approach on the EHA system. The EHA systems consist of a double-rod hydraulic cylinder and a proportional valve that is used to modulate the pressure inside the cylinder.

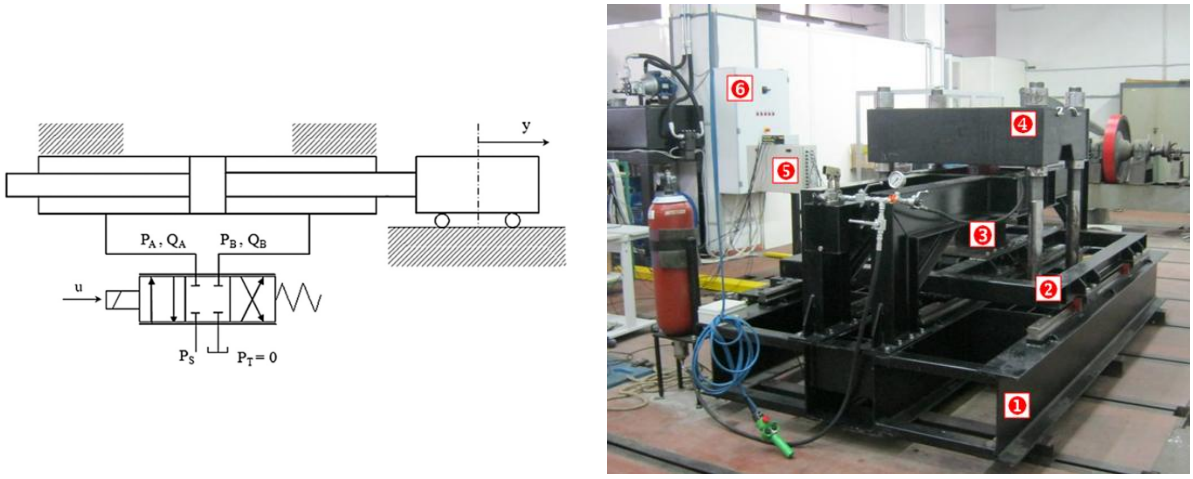

Figure 1: Schematic representation and experimental setup of the hydraulic actuation system [3], [12].

To design the observer, the following mathematical model of EHA is considered [3].

$$
\begin{aligned}
\ddot{y} &= -\frac{b}{m}\dot{y} - \frac{F_f(\dot{y})}{m} + \frac{A_P P_L}{m} \\
\dot{P}_L &= -\frac{2\rho A_P}{V_0}\dot{y} + \frac{2\rho\Psi(v_e)\sqrt{P_S - |P_L|}}{V_0} \\
\ddot{v}_e &= -\omega_{nv}^2 v_e - 2\epsilon_v \omega_{nv}\dot{v}_e + \omega_{nv}^2(k_e u + v_{e0})
\end{aligned}
\tag{1}
$$

where y denotes the position of the piston, $P_L = P_A - P_B$ is the pressure due to the external load and supply, where according to the left-half of Figure 1, P_A and P_B (Q_A and Q_B) are the pressures (the flows) inside the two-cylinder chambers, v_e is the spool valve displacement signal, u is the valve command, b is the viscous friction coefficient, m is the mass of the load, $F_f(\dot{y})$ is the friction force, A_P is the piston area, ρ is the effective bulk modulus, V_0 is the volume of each chamber for the piston centered position, $\Psi(v_e)$ is a gain that depends on the geometry of the adopted proportional valve, P_s and P_T are the supply and tank pressures, respectively, ω_{nv} and ϵ_v are the natural frequency and the damping ratio of the valve, respectively, k_e is the input gain, and v_{e0} represents the spool position bias. In (1), the time variable t is omitted for convenience.

In this paper, only the vector $h\big(t, x(t)\big) = [y \quad P_L \quad v_e]^{\mathrm{T}}$ as the output of the system is measurable and available online. Note that the top, middle, and bottom equations in (1) express the piston rod dynamics, the load pressure dynamics, and the proportional valve dynamics, respectively. Accordingly, the EHA dynamic, based on the proper behavior for each state variable, is divided into three subsystems, and subsequently, three adaptive observers are designed, separately. Hence, $x_1(t) = [y(t), \dot{y}(t)]^{\mathrm{T}} \in R^2$, $x_2(t) = P_L(t) \in R^1$, and $x_3(t) = [v_e(t), \dot{v}_e(t)]^{\mathrm{T}} \in R^2$ are considered as the state vectors; thus the system (1) can be rewritten in state space as,

$$
\begin{bmatrix} \dot{x}_{11} \\ \dot{x}_{12} \end{bmatrix} = \begin{bmatrix} x_{12} \\ -\frac{b}{m}x_{12} + \frac{A_P}{m}x_{21} \end{bmatrix} + \begin{bmatrix} 0 \\ \delta_1 \end{bmatrix}
\tag{2a}
$$

$$\dot{x}_{21} = \frac{2\rho k_q\sqrt{P_s - |x_{21}|}}{V_0}\, x_{31} + \delta_2 \tag{2b}$$

$$\begin{bmatrix} \dot{x}_{31} \\ \dot{x}_{32} \end{bmatrix} = \begin{bmatrix} x_{32} \\ -\omega_{nv}^2\, x_{31} - 2\epsilon_v \omega_{nv}\, x_{32} \end{bmatrix} + k_e \omega_{nv}^2 u \begin{bmatrix} 0 \\ 1 \end{bmatrix} + \begin{bmatrix} 0 \\ \delta_3 \end{bmatrix} \tag{2c}$$

where disturbances are presented as $\delta_1 = \frac{-F_f(x_{12})}{m} + \eta_y(t)$, $\delta_2 = \frac{-2\rho A_P\, x_{12} + 2\rho(\Psi(x_{31}) - k_q\, x_{31})\sqrt{P_s - |x_{21}|}}{V_0} + \eta_{P_L}(t)$, and $\delta_3 = \omega_{nv}^2 v_{e0} + \eta_{v_e}(t)$. In this regard, $\eta = [\eta_y(t) \quad \eta_{P_L}(t) \quad \eta_{v_e}(t)]^T$ includes unmodeled loads, dynamics, and parameter uncertainties. It is worth noticing that due to the unknown terms δ_i, the exact estimation of the full state variables as well as uncertainties in a finite time is not possible, and instead, the ultimate boundedness concept is considered. Before designing the AFFTESO, let us to present the following useful preliminaries:

Proposition 1 [30]: Consider a quadratic positive definite function $\Psi = \mathrm{X}^{\mathrm{T}}\Lambda\mathrm{X}$, where $\mathrm{X} \in \mathcal{R}^n$ and $\Lambda = \Lambda^T \in \mathcal{R}^{n\times n}$ is a real symmetric positive definite matrix. Let $\lambda_{max}(\Lambda)$ and $\lambda_{min}(\Lambda)$ refer to the maximal and minimal eigenvalues of Λ, respectively. If $\|.\|$ denote the Euclidean norm, then for all X

$$\lambda_{\min}(\Lambda)\|\mathrm{X}\|^2 \le \Psi \le \lambda_{\max}(\Lambda)\|\mathrm{X}\|^2 \tag{3}$$

where Λ is a real symmetric positive definite matrix. Besides, by using a straightforward calculation, the variable $\|\mathrm{X}\|$ may be excluded from (3)

$$\lambda_{max}(\Lambda)^{-0.5}\Psi^{0.5} \le \|\mathrm{X}\| \le \lambda_{min}(\Lambda)^{-0.5}\Psi^{0.5} \tag{4}$$

Proposition 2 [31]: Consider the system $\dot{x} = f(x(t))$, where $f: U_0 \to \mathcal{R}^n$ is continuous in an open neighborhood U_0 of the origin. Suppose that this system possesses a unique solution in forwarding time for all initial conditions. Suppose there is a Lyapunov function $V(x)$, positive constants $p_1 \in (0,1)$, $\alpha > 0$, $\beta > 0$, and $\gamma > 0$. Let $V(x_0)$ be the initial value of $V(x)$. Then the following statements hold:

1) If $\dot{V}(x) \le -\alpha V(x)^{p_1} - \beta V(x)$, then the trajectory of the system is fast finite-time stable and the settling time is given by $T \le \frac{ln[1+\beta V(x_0)^{1-p_1}/\alpha]}{\beta(1-p_1)}$.
2) If $\dot{V}(x) \le -\alpha V(x)^{p_1} - \beta V(x) + \gamma V(x)^{p_2}$, where $p_2 < p_1$; then the trajectory of the system is FFTUUB. It means the states x can converge to a region of equilibrium point in a finite time $T \le \frac{ln[1+(\beta-\theta_2)V(x_0)^{1-p_1}/(\alpha-\theta_1)]}{(\beta-\theta_2)(1-p_1)}$, where θ_1 and θ_2 are arbitrary positive constants satisfying $\theta_1 \in (0,\alpha)$ and $\theta_2 \in (0,\beta)$.

3. The Adaptive Fast Finite-Time Extended State Observer (AFFTESO)

In this section, for $i = 1$, 2, and 3, for $j = 1, \dots, n_i$, and for $n_1 = 2$, $n_2 = 1$, and $n_3 = 2$, let $\hat{x}_{ij}$'s be the estimate of x_{ij}'s, and define observation errors as $e_{ij} = \hat{x}_{ij} - x_{ij}$. In the following, AFFTESO (5) is first introduced and Theorem 1 is presented in the absence of uncertainties, which only holds for the nominal model of the EHA system (1). Then, the robustness of the proposed AFFTESO in the presence of these unknowns is analyzed in Theorem 2. Finally, based on the designed AFFTESO (5), the supplementary observer (23) is presented in Theorem 3 that without any knowledge about the upper bounds of the uncertainties is able to provide a finite-time estimation of the total uncertainties. It is worth noting that, the AFFTESOs (5) and (23) are complementary so that together they can estimate the total state variables and uncertainties in a finite time.

$$\dot{\hat{x}}_{ij} = \mathrm{A_i} - \Sigma_i \mathrm{B_i} - (1 - \Sigma_i)\overline{\mathrm{B}}_\mathrm{i} \tag{5}$$

where the adaptive gains Σ_i for $\mathrm{i} = 1,\ 2,$ and 3 are the following switch functions such that $\Sigma_\mathrm{i}: [0, \infty) \to (0,1)$

$$\Sigma_\mathrm{i}(|e_{i1}|) = \begin{cases} 0 + \varepsilon_i & for\ |e_{i1}| \le \tau_i \\ 1 - \varepsilon_i & for\ |e_{i1}| > \tau_i \end{cases} \tag{6}$$

where $\varepsilon_i > 0$ are real constants. Also τ_i are switching thresholds, which influences the convergence rate of the observers. Vectors $\mathrm{A_i}$, $\mathrm{B_i}$, and $\overline{\mathrm{B}}_\mathrm{i}$ for $\mathrm{i} = 1,\ 2,$ and 3 are defined as,

$$\mathrm{A}_1 = \begin{bmatrix} \hat{x}_{12} \\ -\frac{b}{m}\ \hat{x}_{12} + \frac{A_P}{m}\ x_{21} \end{bmatrix}, \quad \mathrm{A}_2 = \frac{2\rho k_q \sqrt{P_S - |\ x_{21}|}}{V_0}\ x_{31}, \quad \mathrm{A}_3 = \begin{bmatrix} \hat{x}_{32} \\ -\omega_{nv}^2\ x_{31} - 2\epsilon_v \omega_{nv}\ \hat{x}_{32} \end{bmatrix} + k_e \omega_{nv}^2 u \begin{bmatrix} 0 \\ 1 \end{bmatrix} \tag{7a}$$

$$\mathrm{B}_1 = \begin{bmatrix} \alpha_{11} sig^{\beta_1}(\ \hat{x}_{11} - x_{11}) \\ \alpha_{12}\left(sig^{2\beta_1 - 1}(\ \hat{x}_{11} - x_{11}) + sig^{\beta_1}(\ \hat{x}_{11} - x_{11})\right) \end{bmatrix}, \qquad \mathrm{B}_2 = \alpha_{21} sig^{\beta_2}(\ \hat{x}_{21} - x_{21}),$$

$$\mathrm{B}_3 = \begin{bmatrix} \alpha_{31} sig^{\beta_3}(\ \hat{x}_{31} - x_{31}) \\ \alpha_{32}\left(sig^{2\beta_3 - 1}(\ \hat{x}_{31} - x_{31}) + sig^{\beta_3}(\ \hat{x}_{31} - x_{31})\right) \end{bmatrix} \tag{7b}$$

$$\overline{\mathrm{B}}_1 = \begin{bmatrix} \alpha_{11}(\ \hat{x}_{11} - x_{11}) \\ \alpha_{12}\left(\ \hat{x}_{11} - x_{11} + sig^{\beta_1}(\ \hat{x}_{11} - x_{11})\right) \end{bmatrix}, \qquad \overline{\mathrm{B}}_2 = \alpha_{21}(\ \hat{x}_{21} - x_{21}),$$

$$\overline{\mathrm{B}}_3 = \begin{bmatrix} \alpha_{31}(\ \hat{x}_{31} - x_{31}) \\ \alpha_{32}\left(\ \hat{x}_{31} - x_{31} + sig^{\beta_3}(\ \hat{x}_{31} - x_{31})\right) \end{bmatrix} \tag{7c}$$

where α_{ij} and $\beta_i \in (0.5,1)$ are appropriate tuning parameters that will be designed later. Also, function $sig^{\overline{\alpha}}(\overline{\overline{\alpha}})$ for constant $\overline{\alpha}$, state $\overline{\overline{\alpha}}$, and the sign function $sign(.)$ is defined as

$$sig^{\overline{\alpha}}(\overline{\overline{\alpha}}) = |\overline{\overline{\alpha}}|^{\overline{\alpha}} sign(\overline{\overline{\alpha}}) \tag{8}$$

According to (2) and (3), the closed-loop system of observation errors are obtained as

$$\begin{bmatrix} \dot{e}_{11} \\ \dot{e}_{12} \end{bmatrix} = \begin{bmatrix} e_{12} \\ -\dfrac{b}{m}\ e_{12} \end{bmatrix} - \Sigma_1 \begin{bmatrix} \alpha_{11} sig^{\beta_1}(e_{11}) \\ \alpha_{12}\left(sig^{2\beta_1 - 1}(e_{11}) + sig^{\beta_1}(e_{11})\right) \end{bmatrix} - (1 - \Sigma_1)\begin{bmatrix} \alpha_{11} e_{11} \\ \alpha_{12}\left(e_{11} + sig^{\beta_1}(e_{11})\right) \end{bmatrix} - \begin{bmatrix} 0 \\ \delta_1 \end{bmatrix} \tag{9a}$$

$$\dot{e}_{21} = -\Sigma_2\left(\alpha_{21} sig^{\beta_2}(e_{21})\right) - (1 - \Sigma_2)\alpha_{21} e_{21} - \delta_2 \tag{9b}$$

$$\begin{bmatrix} \dot{e}_{31} \\ \dot{e}_{32} \end{bmatrix} = \begin{bmatrix} e_{32} \\ -2\epsilon_v \omega_{nv}\, e_{32} \end{bmatrix} - \Sigma_3 \begin{bmatrix} \alpha_{31} sig^{\beta_3}(e_{31}) \\ \alpha_{32}\left(sig^{2\beta_3-1}(e_{31}) + sig^{\beta_3}(e_{31})\right) \end{bmatrix}$$

$$- (1-\Sigma_3) \begin{bmatrix} \alpha_{31} e_{31} \\ \alpha_{32}\left(e_{31} + sig^{\beta_3}(e_{31})\right) \end{bmatrix} - \begin{bmatrix} 0 \\ \delta_3 \end{bmatrix} \tag{9c}$$

The following two theorems are presented in order to prove that the observation errors are respectively fast finite-time stable and/or FFTUUB in the absence or presence of uncertainties δ_i.

Theorem 1: Consider the EHA system (1) and the proposed AFFTESO (5), where the uncertainties (*i.e.* friction force, dead-zone effects of control valves, and spool position bias) and external disturbances are neglected (*i.e.* $\delta_i = 0$). The origin of the closed-loop system of observation errors (9) with $\delta_i = 0$ is fast finite-time stable.

Proof: For convenience, define new state vectors for the first and third subsystems as,

$$\mathrm{E}_i = \left[\Sigma_i sig^{\beta_i}(e_{i1}) + (1-\Sigma_i)e_{i1}, e_{i2}\right]^{\mathrm{T}} \tag{10}$$

where $\mathrm{i} = 1$ and 3, also define a state variable for the second-subsystem as $\mathrm{E}_2 = \Sigma_2 sig^{\beta_2}(e_{21}) + (1-\Sigma_2)e_{21}$. It is clear that, if E_i for $i = 1$, 2, and 3 converge to the zero vector in finite time, then e_{ij} for $i = 1$, 2, and 3, for $j = 1, \dots, n_i$ also converge to the zero vector in finite time. Taking the derivative of E_i for $i = 1$, 2, and 3, the closed-loop system of observation errors (9) are rewritten as

$$\begin{bmatrix} \dot{\mathrm{E}}_{11} \\ \dot{\mathrm{E}}_{12} \end{bmatrix} = |e_{11}|^{\beta_1-1} \begin{bmatrix} -\alpha_{11}\beta_1\Sigma_1 & \beta_1\Sigma_1 \\ -\alpha_{12} & 0 \end{bmatrix} \begin{bmatrix} \mathrm{E}_{11} \\ \mathrm{E}_{12} \end{bmatrix} + \begin{bmatrix} -\alpha_{11}(1-\Sigma_1) & 1-\Sigma_1 \\ -\alpha_{12} & -\frac{b}{m} \end{bmatrix} \begin{bmatrix} \mathrm{E}_{11} \\ \mathrm{E}_{12} \end{bmatrix} \tag{11a}$$

$$\dot{\mathrm{E}}_{21} = -|e_{21}|^{\beta_2-1}\alpha_{21}\beta_2\Sigma_2\mathrm{E}_{21} - \alpha_{21}(1-\Sigma_2)\mathrm{E}_{21} \tag{11b}$$

$$\begin{bmatrix} \dot{\mathrm{E}}_{31} \\ \dot{\mathrm{E}}_{32} \end{bmatrix} = |e_{31}|^{\beta_3-1} \begin{bmatrix} -\alpha_{31}\beta_3\Sigma_3 & \beta_3\Sigma_3 \\ -\alpha_{32} & 0 \end{bmatrix} \begin{bmatrix} \mathrm{E}_{31} \\ \mathrm{E}_{32} \end{bmatrix} + \begin{bmatrix} -\alpha_{31}(1-\Sigma_3) & 1-\Sigma_3 \\ -\alpha_{32} & -2\epsilon_v\omega_{nv} \end{bmatrix} \begin{bmatrix} \mathrm{E}_{31} \\ \mathrm{E}_{32} \end{bmatrix} \tag{11c}$$

where for $i = 1$, 2, and 3, equations (11) can be rewritten as

$$\dot{\mathrm{E}}_i = |e_{i1}|^{\beta_i-1}\mathrm{A}_{i1}^{cl}\mathrm{E}_i + \mathrm{A}_{i2}^{cl}\mathrm{E}_i \tag{12}$$

where $\mathrm{A}_{11}^{cl} = \begin{bmatrix} -\alpha_{11}\beta_1\Sigma_1 & \beta_1\Sigma_1 \\ -\alpha_{12} & 0 \end{bmatrix}$, $\mathrm{A}_{12}^{cl} = \begin{bmatrix} -\alpha_{11}(1-\Sigma_1) & 1-\Sigma_1 \\ -\alpha_{12} & -\frac{b}{m} \end{bmatrix}$, $\mathrm{A}_{21}^{cl} = -\alpha_{21}\beta_2\Sigma_2$, $\mathrm{A}_{22}^{cl} = -\alpha_{21}(1-\Sigma_2)$, $\mathrm{A}_{31}^{cl} = \begin{bmatrix} -\alpha_{31}\beta_3\Sigma_3 & \beta_3\Sigma_3 \\ -\alpha_{32} & 0 \end{bmatrix}$, and $\mathrm{A}_{32}^{cl} = \begin{bmatrix} -\alpha_{31}(1-\Sigma_3) & 1-\Sigma_3 \\ -\alpha_{32} & -2\epsilon_v\omega_{nv} \end{bmatrix}$. Although the compact form (12) is in a matrix format only for subsystems 1 and 3, without loss of generality, the proof is presented for the general matrix form. Since α_{11}, α_{12}, α_{21}, α_{31}, α_{32}, β_i, and $\Sigma_i \in (0,1)$ are positive constants, so A_{i1}^{cl} and A_{i2}^{cl} are Hurwitz matrixes, so there exists symmetric and positive definite matrixes $\mathrm{P}_i = \mathrm{P}_i^{\mathrm{T}}$ such that the following algebraic Lyapunov equations hold

$${\mathrm{A}_{i1}^{cl}}^{\mathrm{T}}\mathrm{P}_i + \mathrm{P}_i\mathrm{A}_{i1}^{cl} = -Q_{i1} \tag{13}$$

$${\mathrm{A}_{i2}^{cl}}^{\mathrm{T}}\mathrm{P}_i + \mathrm{P}_i\mathrm{A}_{i2}^{cl} = -Q_{i2} \tag{14}$$

where $Q_{i1} = Q_{i1}^T$ and $Q_{i2} = Q_{i2}^T$ are arbitrary symmetric and positive definite matrixes. Now, choose a candidate Lyapunov function as $V_i = \mathrm{E}_i^{\mathrm{T}}\mathrm{P}_i\mathrm{E}_i$ and taking its derivative along the systems (11) and (12), we have $\dot{V}_i = \dot{\mathrm{E}}_i^{\mathrm{T}}\mathrm{P}_i\mathrm{E}_i + \mathrm{E}_i^{\mathrm{T}}\mathrm{P}_i\dot{\mathrm{E}}_i$. According to (12), $\dot{\mathrm{E}}_i^{\mathrm{T}} = |e_{i1}|^{\beta_i-1}\mathrm{E}_i^{\mathrm{T}}\mathrm{A}_{i1}^{cl\,\mathrm{T}} + \mathrm{E}_i^{\mathrm{T}}\mathrm{A}_{i2}^{cl\,\mathrm{T}}$; therefore

$$\dot{V}_i = |e_{i1}|^{\beta_i-1}\mathrm{E}_i^{\mathrm{T}}\mathrm{A}_{i1}^{cl\,\mathrm{T}}\mathrm{P}_i\mathrm{E}_i + \mathrm{E}_i^{\mathrm{T}}\mathrm{A}_{i2}^{cl\,\mathrm{T}}\mathrm{P}_i\mathrm{E}_i + |e_{i1}|^{\beta_i-1}\mathrm{E}_i^{\mathrm{T}}\mathrm{P}_i\mathrm{A}_{i1}^{cl}\mathrm{E}_i + \mathrm{E}_i^{\mathrm{T}}\mathrm{P}_i\mathrm{A}_{i2}^{cl}\mathrm{E}_i \tag{15}$$

By using (13) and (14), and with straightforward simplifications, (15) can be rewritten as

$$\dot{V}_i = -|e_{i1}|^{\beta_i-1}\mathrm{E}_i^{\mathrm{T}}Q_{i1}\mathrm{E}_i - \mathrm{E}_i^{\mathrm{T}}Q_{i2}\mathrm{E}_i \tag{16}$$

since $|e_{i1}| \le \|\mathrm{E}_i\|^{1/\beta_i}$ for $\beta_i \in (0.5,1)$, and based on the Proposition 1,

$$\dot{V}_i \le -\lambda_{min}(Q_{i1})\|\mathrm{E}_i\|^{3-1/\beta_i} - \lambda_{min}(Q_{i2})\|\mathrm{E}_i\|^2 \tag{17}$$

Now, by applying Proposition 1 for the candidate Lyapunov function $V_i = \mathrm{E}_i^{\mathrm{T}}\mathrm{P}_i\mathrm{E}_i$, we have

$$\lambda_{max}(\mathrm{P}_i)^{-0.5}V_i^{0.5} \le \|\mathrm{E}_i\| \le \lambda_{min}(\mathrm{P}_i)^{-0.5}V_i^{0.5} \tag{18}$$

therefore

$$\dot{V}_i \le -\gamma_{i1}V_i^{3/2-1/2\beta_i} - \gamma_{i2}V_i \tag{19}$$

where $\gamma_{i1} = \lambda_{min}(Q_{i1})\lambda_{max}(\mathrm{P}_i)^{1/2\beta_i - 3/2}$ and $\gamma_{i2} = \lambda_{min}(Q_{i2})\lambda_{min}(\mathrm{P}_i)^{-1}$. By selecting the parameter $\beta_i \in (0.5,1)$, it results that $3/2 - 1/2\beta_i > 1/2$. Therefore, based on Proposition 2, the origin of the observation errors dynamic system (9) in the absence of uncertainties is fast finite-time stable, and the settling time is given by $T \le 2ln\left[1 + \gamma_{i2}V_{i-0}^{1/2+1/2\beta_i}/\gamma_{i1}\right]\left[\gamma_{i2}\left(-1 + \beta_i^{-1}\right)\right]^{-1}$, where V_{i-0} are the initial value of V_i. Thus, the arguments stated in Theorem 1 hold, and hence the proof is completed.☐

The above theorem only holds for the nominal model of EHA system (1), but since uncertainties and external disturbances always exist in real applications, the robustness of the proposed adaptive fast finite-time observer in the presence of these unknowns are now analyzed.

Theorem 2: Consider the EHA system (1) and the proposed AFFTESO (5) in the presence of uncertainties (*i.e.* friction force, dead-zone effects of control valves, and spool position bias) and external disturbances. The origin of the closed-loop system of observation errors (9) is FFTUUB.

Proof: In this proof, the analysis procedure is given along the similar analysis outlined in the proof of theorem 1, except the appearance of the uncertainties. Define the new state vectors E_i, which are the same as (10) and $\mathrm{E}_2 = \Sigma_2 sig^{\beta_2}(e_{21}) + (1-\Sigma_2)e_{21}$. By considering the uncertainties and taking the derivative of E_i, the differential equation (12) is rewritten as

$$\dot{\mathrm{E}}_i = |e_{i1}|^{\beta_i-1}\mathrm{A}_{i1}^{cl}\mathrm{E}_i + \mathrm{A}_{i2}^{cl}\mathrm{E}_i + \Delta_i \tag{20}$$

where $\Delta_1 = -\begin{bmatrix} 0 \\ \delta_1 \end{bmatrix}$, $\Delta_2 = -|e_{21}|^{\beta_2-1}\beta_2\Sigma_2\delta_2 - (1-\Sigma_2)\delta_2$, and $\Delta_3 = -\begin{bmatrix} 0 \\ \delta_3 \end{bmatrix}$, so that the following assumption is considered.

Assumption 1: The unknown terms Δ_i are bounded. Thus, there exists positive constants ϱ_i such that $\|\Delta_i\| \le \varrho_i$.

Now, by using the candidate Lyapunov functions $V_i = \mathrm{E}_i{}^{\mathrm{T}}\mathrm{P}_i\mathrm{E}_i$ and taking its derivative along the systems (20), we have

$$\dot{V}_i = |e_{i1}|^{\beta_i-1}\mathrm{E}_i{}^{\mathrm{T}}\mathrm{A}_{i1}^{cl}{}^{\mathrm{T}}\mathrm{P}_i\mathrm{E}_i + \mathrm{E}_i{}^{\mathrm{T}}\mathrm{A}_{i2}^{cl}{}^{\mathrm{T}}\mathrm{P}_i\mathrm{E}_i + \Delta_i{}^{\mathrm{T}}\mathrm{P}_i\mathrm{E}_i + |e_{i1}|^{\beta_i-1}\mathrm{E}_i{}^{\mathrm{T}}\mathrm{P}_i\mathrm{A}_{i1}^{cl}\mathrm{E}_i + \mathrm{E}_i{}^{\mathrm{T}}\mathrm{P}_i\mathrm{A}_{i2}^{cl}\mathrm{E}_i + \mathrm{E}_i{}^{\mathrm{T}}\mathrm{P}_i\Delta_i \tag{21}$$

where by using (13) and (14), (21) can be rewritten as

$$\dot{V}_i = -|e_{i1}|^{\beta_i-1}\mathrm{E}_i{}^{\mathrm{T}}Q_{i1}\mathrm{E}_i - \mathrm{E}_i{}^{\mathrm{T}}Q_{i2}\mathrm{E}_i + 2\mathrm{E}_i{}^{\mathrm{T}}\mathrm{P}_i\Delta_i \tag{22}$$

Since $|e_{i1}| \le \|\mathrm{E}_i\|^{1/\beta_i}$ for $\beta_i \in (0.5,1)$, therefore based on the Proposition 1 and assumption 1, we have

$$\dot{V}_i \le -\lambda_{min}(Q_{i1})\|\mathrm{E}_i\|^{3-1/\beta_i} - \lambda_{min}(Q_{i2})\|\mathrm{E}_i\|^2 + 2\|\mathrm{E}_i\|\|\mathrm{P}_i\|\varrho_i \tag{23}$$

after some straightforward calculations, these upper bound are given by,

$$\dot{V}_i \le -\gamma_{i1}V_i^{3/2-1/2\beta_i} - \gamma_{i2}V_i + \gamma_{i3}V_i^{0.5} \tag{24}$$

where $\gamma_{i3} = 2\|\mathrm{P}_i\|\varrho_i\lambda_{min}(\mathrm{P}_i)^{-0.5}$. Therefore based on Proposition 2, the origin of the observation errors dynamic system (9) in the presence of uncertainties is FFTUUB. It means the estimation errors can converge to a region of equilibrium point in a finite time $T \le \frac{ln\left[1+(\gamma_{i2}-\theta_2)V(x_0)^{1/2+1/2\beta_i}/(\gamma_{i1}-\theta_1)\right]}{(\gamma_{i2}-\theta_2)(1-p_1)}$, where θ_1 and θ_2 are arbitrary positive constants satisfying $\theta_1 \in (0,\gamma_{i1})$ and $\theta_2 \in (0,\gamma_{i2})$. Thus, the arguments stated in Theorem 2 hold, and hence the proof is completed.□

So far, the stability analysis of the proposed AFFTESO (5) has been presented, where observation errors convergence to a neighborhood of zero in a finite time has been proved in the presence of uncertainties and external disturbances. Now, based on the designed AFFTESO (5), a supplementary AFFTESO able to provide finite-time estimation of the total uncertainties is introduced.

$$\dot{\hat{\delta}}_i = -\bar{\alpha}_{i(n_i+1)}\bar{\Sigma}_i\left(sig^{2\bar{\beta}_i-1}(e_i) + sig^{\bar{\beta}_i}(e_i)\right) - \bar{\alpha}_{i(n_i+1)}(1-\bar{\Sigma}_i)\left(e_i + sig^{\bar{\beta}_i}(e_i)\right) \tag{25}$$

where $e_1 = \hat{\hat{x}}_{12} - \hat{x}_{12}$, $e_2 = e_{21} = \hat{x}_{21} - x_{21}$, and $e_3 = \hat{\hat{x}}_{32} - \hat{x}_{32}$, in which $\hat{x}$ is obtained by the state observer (5) and $\hat{\hat{x}}$'s represent new estimations of the estimated states $\hat{x}$ that will be defined later. In the following theorem, it is discussed that without any knowledge about the upper bounds of the uncertainties, the adaptive observer (25) can estimate the total uncertainties in a finite time.

Theorem 3: Consider the EHA system (1), the proposed AFFTESO (5), and supplementary adaptive fast finite-time observer (25), where the uncertainties satisfy the Lipschitz-like conditions $|\dot{\delta}_1| < \sigma_1$, $|\dot{\delta}_2| < \sigma_2$, and $|\dot{\delta}_3| < \sigma_3$. The states $\hat{\delta}_i$ of the observer (25) will fast finite-time converge to a small neighborhood of the real states δ_i.

Proof: Based on the stability analysis of the proposed state observer (5) it can be concluded that the acceptable robust estimates of the state variables is already obtained in a finite time. First by using the estimations obtained from the state observer (5) the EHA model can be rewritten as follow,

$$\dot{x}_{12} = -\frac{b}{m}\hat{x}_{12} + \frac{A_P}{m}\, x_{21} + \frac{b}{m}e_{12} + \delta_1 \tag{26a}$$

$$\dot{x}_{21} = \frac{2\rho k_q\sqrt{P_s - |\, x_{21}|}}{V_0}\, x_{31} + \delta_2 \tag{26b}$$

$$\dot{x}_{32} = -\omega_{nv}^2\, x_{31} - 2\epsilon_v\omega_{nv}\,\hat{x}_{32} + k_e\omega_{nv}^2 u + 2\epsilon_v\omega_{nv}\, e_{32} + \delta_3 \tag{26c}$$

According to (25), $e_1 = \hat{\hat{x}}_{12} - \hat{x}_{12}$ and $e_3 = \hat{\hat{x}}_{32} - \hat{x}_{32}$, where $\hat{\hat{x}}_{12}$ and $\hat{\hat{x}}_{32}$ are new estimations of the estimated states $\hat{x}$ that are obtained by,

$$\dot{\hat{\hat{x}}}_{12} = -\frac{b}{m}\,\hat{x}_{12} + \frac{A_P}{m}x_{21} + \hat{\delta}_1 - \bar{\alpha}_{12}\bar{\Sigma}_1\left(sig^{2\bar{\beta}_1 - 1}(e_1) + sig^{\bar{\beta}_1}(e_1)\right) - \bar{\alpha}_{12}(1 - \bar{\Sigma}_1)\left(e_1 + sig^{\bar{\beta}_1}(e_1)\right) \tag{27a}$$

$$\dot{\hat{\hat{x}}}_{32} = -\omega_{nv}^2\, x_{31} - 2\epsilon_v\omega_{nv}\,\hat{x}_{32} + \hat{\delta}_3 - \bar{\alpha}_{32}\bar{\Sigma}_3\left(sig^{2\bar{\beta}_3 - 1}(e_3) + sig^{\bar{\beta}_3}(e_3)\right) - \bar{\alpha}_{32}(1 - \bar{\Sigma}_3)\left(e_3 + sig^{\bar{\beta}_3}(e_3)\right) \tag{27b}$$

where $\hat{x}_{12}$, $\hat{x}_{32}$ and $\hat{\delta}_1$, $\hat{\delta}_3$ are respectively updated by (5) and (25). According to (25), (27), e_i and $e_{\delta_i} = \hat{\delta}_i - \delta_i$ ($i = 1$, 2, and 3), let define new observation error vectors as

$$\mathrm{E}_{\delta i} = \left[\bar{\Sigma}_i sig^{\bar{\beta}_i}(e_i) + (1 - \bar{\Sigma}_i)e_i, e_{\delta_i}\right]^{\mathrm{T}} \tag{28}$$

It is clear that, if $\mathrm{E}_{\delta i}$ for $i = 1$, 2, and 3 converge to the zero vector in finite time, then e_i and e_{δ_i} also converge to the zero vector in finite time. Taking the derivative of $\mathrm{E}_{\delta i}$ for $i = 1$, 2, and 3, the following closed-loop system of the new observation errors (28) are obtained.

$$\dot{\mathrm{E}}_{\delta i} = |e_i|^{\bar{\beta}_i - 1}\bar{\mathrm{A}}_{i1}^{cl}\mathrm{E}_{\delta i} + \bar{\mathrm{A}}_{i2}^{cl}\mathrm{E}_{\delta i} + \bar{\Delta}_i \tag{29}$$

where $\bar{\mathrm{A}}_{i1}^{cl} = \begin{bmatrix} -\bar{\alpha}_{in_i}\bar{\beta}_i\bar{\Sigma}_i & \bar{\beta}_i\bar{\Sigma}_i \\ -\bar{\alpha}_{i(n_i+1)} & 0 \end{bmatrix}$, $\bar{\mathrm{A}}_{i2}^{cl} = \begin{bmatrix} -\bar{\alpha}_{in_i}(1 - \bar{\Sigma}_i) & 1 - \bar{\Sigma}_i \\ -\bar{\alpha}_{i(n_i+1)} & 0 \end{bmatrix}$, and $\bar{\Delta}_i = \left(|e_i|^{\bar{\beta}_i - 1}\begin{bmatrix} \bar{\beta}_i\bar{\Sigma}_i \\ 0 \end{bmatrix} + \begin{bmatrix} 1 - \bar{\Sigma}_i \\ 0 \end{bmatrix}\right)\Pi_i - \begin{bmatrix} 0 \\ 1 \end{bmatrix} S_i$ in which $\Pi_1 = \frac{b}{m}e_{12}$, $\Pi_2 = 0$, $\Pi_3 = 2\epsilon_v\omega_{nv}\, e_{32}$, and $\dot{\delta}_i = S_i$. Since $\bar{\mathrm{A}}_{i1}^{cl}$ and $\bar{\mathrm{A}}_{i2}^{cl}$ are Hurwitz matrixes, so there exists symmetric and positive definite matrixes $\bar{\mathrm{P}}_i = \bar{\mathrm{P}}_i^{\mathrm{T}}$ such that the following algebraic Lyapunov equations hold

$$\bar{\mathrm{A}}_{i1}^{cl\,\mathrm{T}}\bar{\mathrm{P}}_i + \bar{\mathrm{P}}_i\bar{\mathrm{A}}_{i1}^{cl} = -\bar{Q}_{i1} \tag{30}$$

$$\bar{\mathrm{A}}_{i2}^{cl\,\mathrm{T}}\bar{\mathrm{P}}_i + \bar{\mathrm{P}}_i\bar{\mathrm{A}}_{i2}^{cl} = -\bar{Q}_{i2} \tag{31}$$

where $\bar{Q}_{i1}$ and $\bar{Q}_{i2}$ are arbitrary symmetric and positive definite matrixes. By using new candidate Lyapunov functions $\bar{V}_i = \mathrm{E}_{\delta i}{}^{\mathrm{T}}\bar{\mathrm{P}}_i\mathrm{E}_{\delta i}$ and taking its derivative along the dynamic (29), we have

$$\dot{\bar{V}}_i = |e_i|^{\bar{\beta}_i - 1}\mathrm{E}_{\delta i}{}^{\mathrm{T}}\bar{\mathrm{A}}_{i1}^{cl\,\mathrm{T}}\bar{\mathrm{P}}_i\mathrm{E}_{\delta i} + \mathrm{E}_{\delta i}{}^{\mathrm{T}}\bar{\mathrm{A}}_{i2}^{cl\,\mathrm{T}}\bar{\mathrm{P}}_i\mathrm{E}_{\delta i} + \bar{\Delta}_i{}^{\mathrm{T}}\bar{\mathrm{P}}_i\mathrm{E}_{\delta i} + |e_i|^{\beta_i - 1}\mathrm{E}_{\delta i}{}^{\mathrm{T}}\bar{\mathrm{P}}_i\bar{\mathrm{A}}_{i1}^{cl}\mathrm{E}_{\delta i} + \mathrm{E}_{\delta i}{}^{\mathrm{T}}\bar{\mathrm{P}}_i\bar{\mathrm{A}}_{i2}^{cl}\mathrm{E}_{\delta i} + \mathrm{E}_{\delta i}{}^{\mathrm{T}}\bar{\mathrm{P}}_i\bar{\Delta}_i \tag{32}$$

where by using (30) and (31), (32) can be rewritten as

$$\dot{\bar{V}}_i = -|e_i|^{\bar{\beta}_i - 1}\mathrm{E}_{\delta i}{}^{\mathrm{T}}\bar{Q}_{i1}\mathrm{E}_{\delta i} - \mathrm{E}_{\delta i}{}^{\mathrm{T}}\bar{Q}_{i2}\mathrm{E}_{\delta i} + 2\mathrm{E}_{\delta i}{}^{\mathrm{T}}\bar{\mathrm{P}}_i\bar{\Delta}_i \tag{33}$$

Based on the Proposition 1 and an assumption that $\|\bar{\Delta}_i\| \leq \bar{\varrho}_i$, we have

$$\dot{\bar{V}}_i \leq -\lambda_{min}(\bar{Q}_{i1})\|\mathrm{E}_{\delta i}\|^{3-1/\bar{\beta}_i} - \lambda_{min}(\bar{Q}_{i2})\|\mathrm{E}_{\delta i}\|^2 + 2\|\mathrm{E}_{\delta i}\|\|\bar{\mathrm{P}}_i\|\bar{\varrho}_i \tag{34}$$

after some straightforward calculations, these upper bound are given by,

$$\dot{\bar{V}}_i \leq -\bar{\gamma}_{i1}\bar{V}_i^{3/2 - 1/2\bar{\beta}_i} - \bar{\gamma}_{i2}\bar{V}_i + \bar{\gamma}_{i3}\bar{V}_i^{0.5} \tag{35}$$

where $\bar{\gamma}_{i1} = \lambda_{min}(\bar{Q}_{i1})\lambda_{max}(\bar{\mathrm{P}}_i)^{1/2\bar{\beta}_i - 3/2}$, $\bar{\gamma}_{i2} = \lambda_{min}(\bar{Q}_{i2})\lambda_{min}(\bar{\mathrm{P}}_i)^{-1}$, and $\bar{\gamma}_{i3} = 2\|\bar{\mathrm{P}}_i\|\bar{\varrho}_i\lambda_{min}(\bar{\mathrm{P}}_i)^{-0.5}$. Therefore, based on Proposition 2, the origin of the new observation errors dynamics (29) in the presence of uncertainties is FFTUUB, hence the states $\hat{\delta}_i$ of the observer (25) will finite-time converge to the real states δ_i. Thus, the arguments stated in Theorem 3 hold, and hence the proof is completed.☐

Remark 1: According to $\bar{\Delta}_i$, since Π_i and S_i are bounded, therefore the assumption $\|\bar{\Delta}_i\| \leq \bar{\varrho}_i$ is approved.

Remark 2: In this paper, the suggested adaptive framework based on the switch function Σ_i can improve the convergence rate for zones both far from the equilibrium points and around them. In this regard, the adaptive gains are computed based on the evaluation of the absolute value of the observation errors, achieving finite-time estimate of both the full state variables as well as uncertainties.

Remark 3: In terms of limitations of the proposed method in real applications, the proposed scheme is straightforward to design and implement. Its construction relies only on choosing the positive real constants ε_i, τ_i, α_{ij}, $\bar{\alpha}_{ij}$, and $\beta_i \in (0.5,1)$. On the other hand, the AFFTESO (5) and its gains have been computed based on some ordinary algebraic equations, which can be implemented on usual hardware and it will not need powerful processors. Moreover, according to the block diagram in Figure 17, the proposed observers is designed using only the vector $h(t, x(t)) = [y \quad P_L \quad v_e]^T$ as the output of the system that is measurable and available online.

4. Simulation, analysis, and experimental validation

In this section, to validate the effectiveness of the proposed AFFTESO (5) and (25), simulations are presented for the uncertain EHA system (1), and experimental results are obtained using the electro-hydraulic test-bed system in Figure 1. All the considered observers are designed based on the nominal explicit parameters provided in Table 1 and for the positive real constants $\varepsilon_i = 0.2$ and $\beta_i = 0.8$ for $i = 1,2,3$, and $\tau_1 = 0.0003$, $\tau_2 = 4000$, $\tau_1 = 0.4$, and $\alpha_{ij} = \bar{\alpha}_{ij}$, where $\alpha_{11} = \alpha_{21} = \alpha_{31} = 50 = 50$, $\alpha_{12} = \alpha_{22} = \alpha_{32} = 20\alpha_{11}$. Also, since the presented scheme is not a fixed-time observer, which convergence of the estimation errors to a small neighborhood of zero is achieved regardless of the initial conditions, hence the change in convergence time from the initial conditions is evident. Therefore, all results are illustrated with zero initial conditions. Besides, to understand the dead-zone's effects in the simulation and experimental comparative studies, the valve command input signal are the ones plotted in Figure 2.

Table 1

Nominal parameters of the hydraulic actuator [3]

	Symbol	Unit	Value
Piston mass	m	kg	440
Piston area	b	m^2	0.01
Centered camera volume	V_0	m^3	0.004
Bulk modulus	ρ	Pa	1e9
Input gain	k_e	-	0.49
Valve natural frequency	ω_{nv}	s^{-1}	152
Valve damping coefficient	ϵ_v	-	0.92
Supply pressure	P_s	Pa	1e7

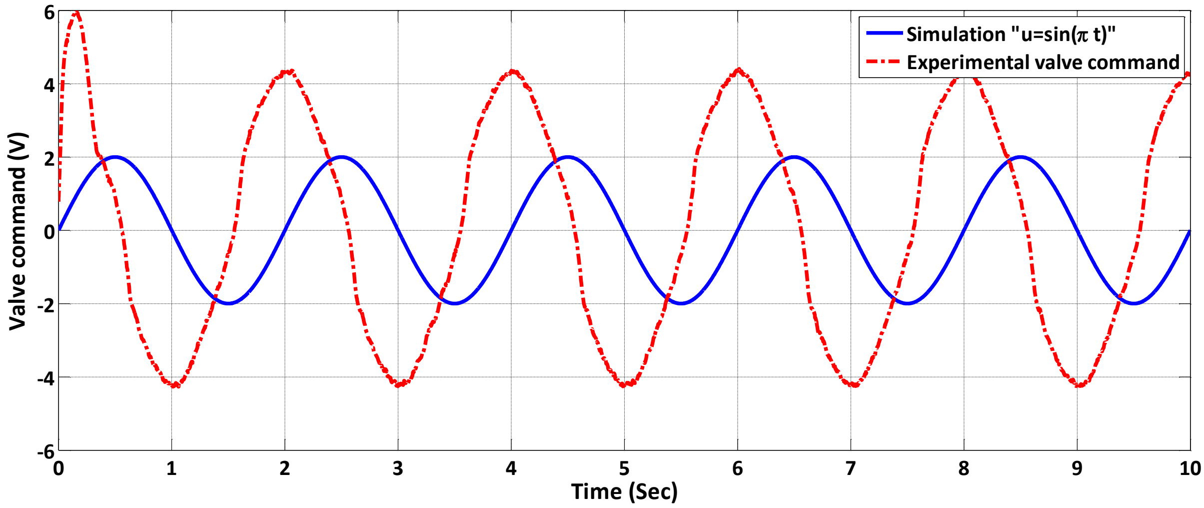

Figure 2. Valve command input voltage adopted for all the simulation and experimental tests.

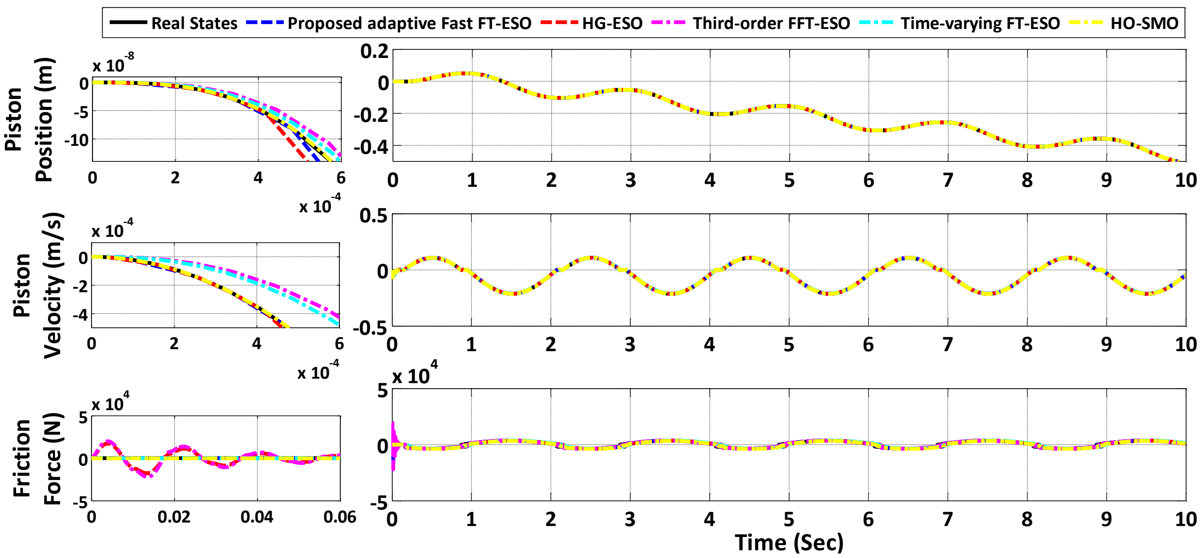

Figure 3. Real states and estimation results of the first-subsystem.

First, comparative simulations are reported in Figures 3-5 to highlight the efficiency of the proposed AFFTESO (adaptive fast FT-ESO) with respect to four leading strategies HG-ESO in [21, 22], third-order FFTESO in [20], time-varying FT-ESO in [29], and HO-SMO in [12]. In response to the considered valve command signal, one can find from Figure 3 that by employing the proposed AFFTESO, the piston position and velocity variables remain at a small neighborhood of the real states in a finite time and in the presence of friction force, while this uncertain variable is observed simultaneously. It can be seen that the proposed AFFTESO can achieve higher observation accuracy and faster convergence speed. According to the Figure 3, three methods, such as AFFTESO, HG-ESO, and HO-SMO, are able to provide better finite-time estimations of the full state variables as well as the friction force compared to the third-order FFTESO and time-varying FT-ESO methods. By defining the root mean square (RMS) performance index for $i = 1, 2, 3$ and $j = 1, \dots, n_i + 1$ as

$$J_i = \left\| \sqrt{\frac{1}{t_s} \int_0^{t_s} e_{ij}^T e_{ij} \, dt} \right\| \tag{36}$$

where for $i = 1$, J_1 with physical unit $[m, {}^{m}/_{s}, N]^T$ that expressed based on the infinity norm of the observation error vector of the first-subsystem, the performance of all studied observers will be evaluated in Table 2. For the purpose of fair comparison, the parameters of studied observers are adjusted in order to achieve the best observation results. Moreover, the EHA system studied in [3] is now considered, where the second-subsystem is affected by uncertainties coming from subsystems 1 and 3. To show the robustness of the proposed AFFTESO against the state dependent uncertainties (Dead-Zone effects), Figure 4 is presented, while the corresponding valve command signal is reported in Figure 2. Figure 4 shows that the proposed observer ensures a better convergence time compared to the HGESO, third-order FFTESO, time-varying FT-ESO, and HO-SMO. Moreover, it is able to provide more acceptable finite-time estimations of the full state variables as well as the Dead-Zone effects.

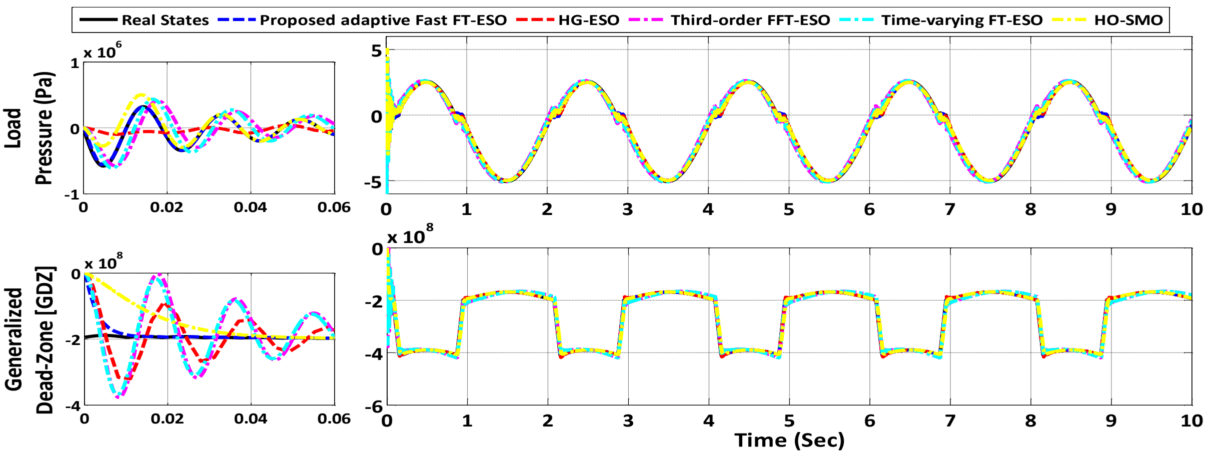

Figure 4. Real states and estimation results of the second-subsystem.

It is worth noting that, in this paper $\Psi(v_e) = \Psi(x_{31})$ represents the dead-zone effects, while $\delta_2 = \frac{-2\rho A_P x_{12} + 2\rho(\Psi(x_{31}) - k_q x_{31})\sqrt{P_S - |x_{21}|}}{V_0} + \eta_{P_L}(t)$ represents the generalized dead-zone effects that include unmodeled dynamics and dead-zone effects. Now, according to (36) for $i = 2$ by defining the RMS performance index J_2 with physical unit $\left[Pa, {m^3}/{s\, Pa^{\frac{1}{2}}}\right]^T$ that expressed based on the infinity norm of the observation error vector of the second-subsystem, the performance of all studied observers are reported in Table 2.

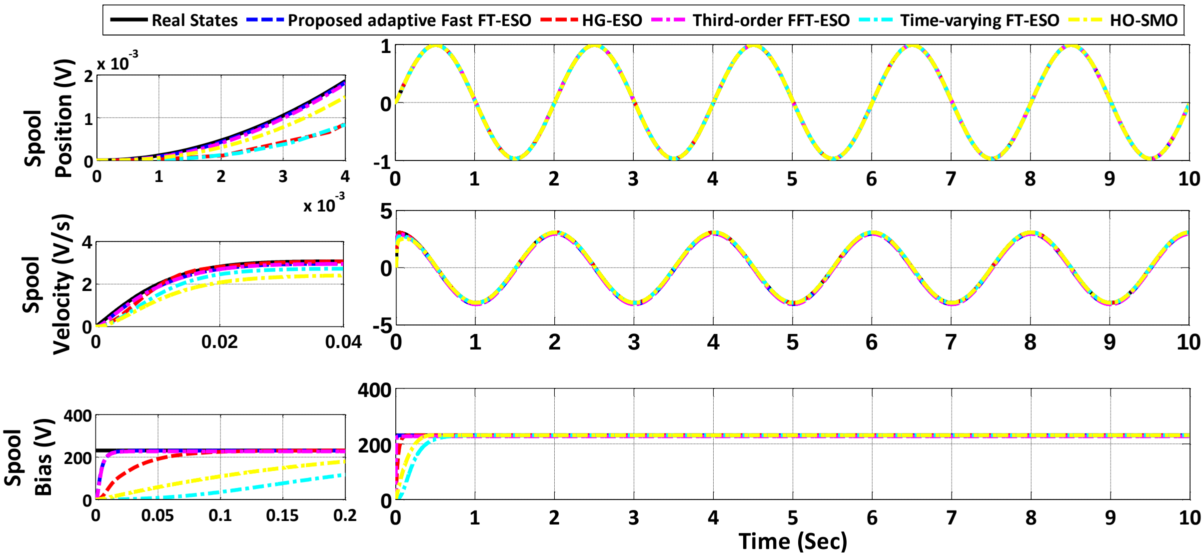

Figure 5. Real states and estimation results of the third-subsystem.

According to Figure 5, the proposed AFFTESO could satisfy not only the state observation error constraints on the steady-state observation errors but also this constraint on the observation error for uncertainties, where the finite-time convergence is guaranteed without any knowledge about their upper bounds. Finally, according to (36) for $i = 3$ by defining the RMS performance index J_3 with physical unit $[V, {V}/{s}, V]^T$ that expressed based on the infinity norm of the observation error vector of the third-subsystem, the performance of all studied observers is evaluated in Table 2. It is worth noting that, computing the L_2 norm of the estimation error vector does not make sense, because each element has a dissimilar magnitude (or range) along with a different physical unit, where L_2 norms of the estimation error vector are clearly dominated by the last elements and naturally, the measure would disregard the smaller elements. Therefore, the vector elements are handled and are compared individually to the corresponding ones among competing methods. According to Table 2, the first element of the RMS performance index J_1 obtained by the proposed AFFTESO has the L_2 norm 10.19×10^{-11}, where the HG-ESO, third-order FFTESO, time-varying FT-ESO, and HO-SMO have the L_2 norm 5.35×10^{-11}, 4.01×10^{-4}, 2.43×10^{-4}, and 3.86×10^{-11}, respectively. Also, the second element of the RMS performance index J_1 obtained by the proposed AFFTESO has the L_2 norm 9.5×10^{-4}, where the HG-ESO, third-order FFTESO, time-varying FT-ESO, and HO-SMO have the L_2 norm 14.79×10^{-4}, 0.38, 0.16, and 10.94×10^{-4}, respectively. According to the first two elements and the third element, it is concluded that in spite of a better performance of the first element of J_1 of the HG-ESO and HO-SMO approaches, the proposed AFFTESO has a better performance in terms of estimation in the presence of uncertainties. Besides, in Table 2 we can appreciate the behavior of the same RMS performance index in the load pressure estimation but enlarging a portion of the behavior in Dead-Zone effects estimation is evident. According to the results of the RMS performance index J_2, it can be concluded that the proposed AFFTESO has more than 70% better performance compared to the studied approaches in terms of estimation in the presence of uncertainties.

Table 2

Comparative results between the performance indexes.

	J_1 with physical unit $[m, {}^{m}/_{s}, N]^T$	J_2 with physical unit $\left[Pa, {}^{m^3}/_{s\,Pa^{\frac{1}{2}}}\right]^T$	J_3 with physical unit $\left[V, {}^{V}/_{s}, V\right]^T$
Proposed adaptive fast FT-ESO (AFFTESO)	$\begin{bmatrix} 10.19 \times 10^{-11} \\ 9.50 \times 10^{-4} \\ 10.47 \end{bmatrix}$	$\begin{bmatrix} 1.10 \\ 21320 \end{bmatrix} \times 10^{14}$	$\begin{bmatrix} 1.57 \\ 0.20 \times 10^{4} \\ 4.58 \times 10^{7} \end{bmatrix}$
HG-ESO [21]	$\begin{bmatrix} 5.35 \times 10^{-11} \\ 14.79 \times 10^{-4} \\ 18.48 \end{bmatrix}$	$\begin{bmatrix} 1.47 \\ 107020 \end{bmatrix} \times 10^{14}$	$\begin{bmatrix} 9.16 \\ 2.26 \times 10^{4} \\ 7.93 \times 10^{7} \end{bmatrix}$
Third-order FFTESO [20]	$\begin{bmatrix} 4.01 \times 10^{-4} \\ 0.38 \\ 320.67 \end{bmatrix}$	$\begin{bmatrix} 1.52 \\ 301780 \end{bmatrix} \times 10^{14}$	$\begin{bmatrix} 1.07 \\ 0.41 \times 10^{4} \\ 10.09 \times 10^{7} \end{bmatrix}$
Time-varying FT-ESO [29]	$\begin{bmatrix} 2.43 \times 10^{-4} \\ 0.16 \\ 160.24 \end{bmatrix}$	$\begin{bmatrix} 1.50 \\ 265510 \end{bmatrix} \times 10^{14}$	$\begin{bmatrix} 6.60 \\ 2.13 \times 10^{4} \\ 10.22 \times 10^{7} \end{bmatrix}$
HO-SMO [12]	$\begin{bmatrix} 3.86 \times 10^{-11} \\ 10.94 \times 10^{-4} \\ 12.55 \end{bmatrix}$	$\begin{bmatrix} 1.67 \\ 70890 \end{bmatrix} \times 10^{14}$	$\begin{bmatrix} 2.57 \\ 0.40 \times 10^{4} \\ 10.27 \times 10^{7} \end{bmatrix}$

Furthermore, according to Table 2, it can be noted that the estimations of the position and velocity of the spool have nice behaviors and are almost independent of the high spool bias. The first elements of the RMS performance index J_3 obtained using the proposed AFFTESO has the L_2 norm 1.57, where the HG-ESO, third-order FFTESO, time-varying FT-ESO, and HO-SMO have the L_2 norm 9.16, 1.07, 6.6, and 2.57, respectively. Although, the results of the third-order FFTESO approach is better than the proposed AFFTESO, its performance is not always praiseworthy which the other elements of J_3 show this fact. In this regard, the second elements of the RMS performance indexJ_3 obtained using the proposed AFFTESO has the L_2 norm 0.2×10^4, where the HG-ESO, third-order FFTESO, time-varying FT-ESO, and HO-SMO have the L_2 norm 2.26×10^4, 0.41×10^4, 2.13×10^4, and 0.40×10^4, respectively. It can be concluded that, in the presence of unknown terms such as external disturbances and spool bias, the ultimate boundedness concept is achieved, while a negligible steady-state error is reached for the variables. Thus, the proposed approach represents a valid alternative way to design the finite-time observers. According to the presented theorems, the gains Σ_i for $i = 1$, 2, and 3 are adaptive positive gains. Now the validation of the proposed adaptive-gain strategy compared with the fixed-gain case is performed in simulations.

5.1. Comparison of different classes of adaptive and fixed gain observer

Different from the traditional HGESO, third-order FFTESO, and HO-SMO designs, in this paper we use the new adaptive gains Σ_i's instead of constant gains, where the studied finite-time observers with function $sign(.)$ only have a faster convergence rate around the equilibrium points and demonstrate a slower convergence rate far from the equilibrium points. The proposed AFFTESO with the new adaptive gains Σ_i's can avoid this problem, where the gains Σ_i's are changed based on the evaluation of the absolute value of the observation errors. It is worth noting that, depending on the value of the triggers τ_i and the gains ε_i for $i = 1$, 2, and 3, there has been a trade-off between convergence rate around the equilibrium points and far from of them. The following results are now presented to demonstrate the effectiveness of the proposed adaptive framework, in which comparison simulations between AFFTESO (adaptive fast FTESO) and fixed-gain fast FTESO schemes are presented. In fact, this subsection is only provided to show positive effects of the adaptive framework.

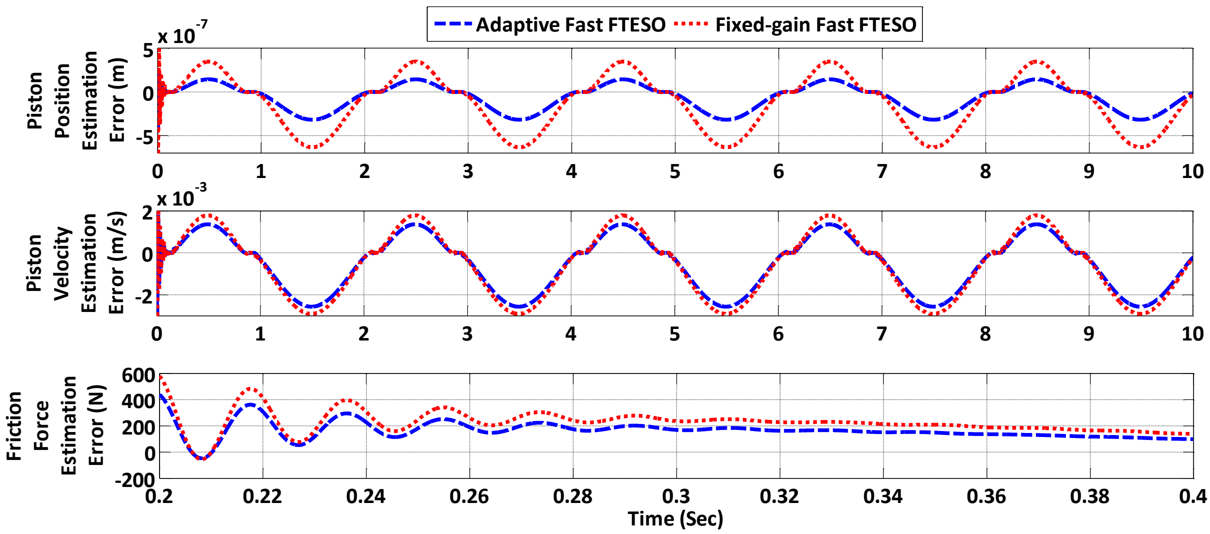

Figure 6. Estimation errors of the first-subsystem under adaptive and fixed gains.

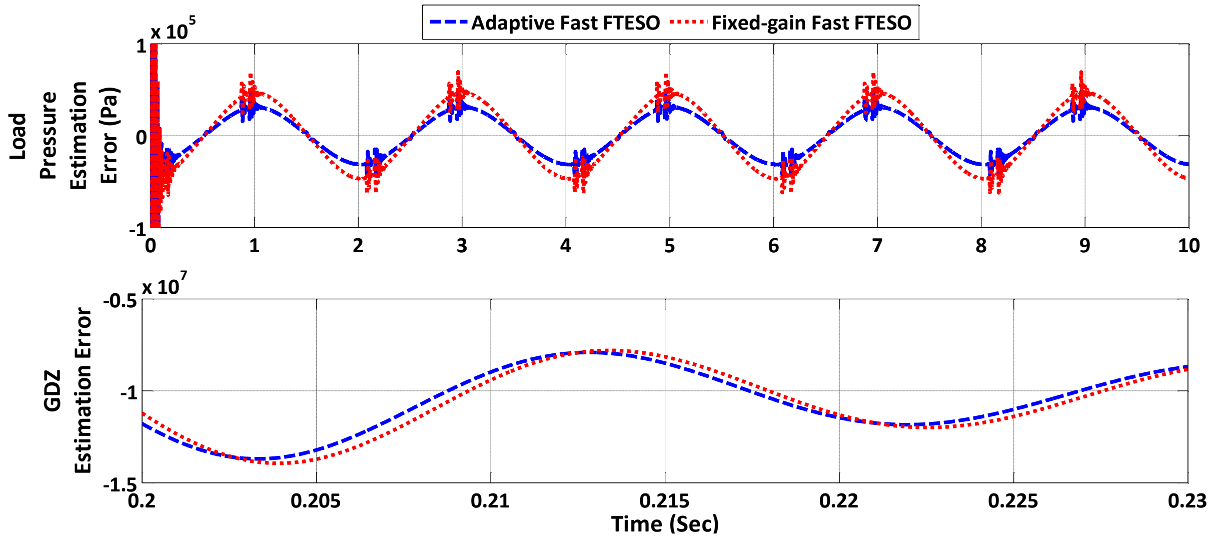

Figure 7. Estimation errors of the second-subsystem under adaptive and fixed gains.

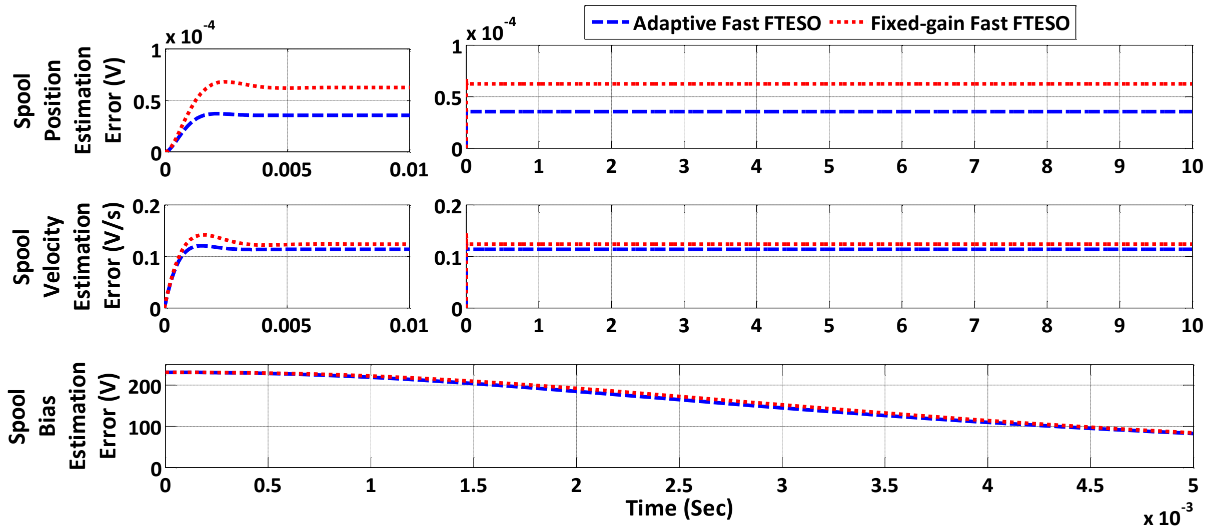

Figure 8. Estimation errors of the third-subsystem under adaptive and fixed gains.

From Figures 6-8 it can be detected correctly that the observation errors corresponding to the proposed AFFTESO is less than the one with fixed gains, which implies that the adaptive framework an lead to much more sensitivity to the observation errors. Also, it is explored that with the application of new adaptive gains Σ_i's instead of constant gains, the estimation errors experience a better performance. In contrast, the outcomes reveal that with the proposed AFFTESO, the estimation errors are reduced and better satisfy the steady-state requirements than the other considered approaches. Therefore, it can be concluded that, the proposed scheme can compete with the other leading strategies, which makes it a qualified alternative approach in the observer design with noteworthy potential. Up to now, the proposed AFFTESO performs better with the adaptive gain compared to the simple gain function. Hence, we use the adaptive gain for further experiments. To validate the feasibility of the proposed approach against the real-world conditions, the following experimental studies are sketched in Figures 9-16, where are the results of one of several successful experimental runs.

5.2. Experimental Results

In this section, experimental results are obtained using the EHA test-bed shown in the right-half of Figure 1, where the setup is equipped with sensors providing measurements of output variables y, P_L, and v_e. Besides, to the comparison with the data estimated by the observers, these practical data are first reconstructed through digital filtering. In this paper, to validate the effectiveness of the proposed AFFTESO in a real-life scenario, an experiment in presence of a load connected to the sliding table is performed, where according to the right-half of Figure 1, the markers 1 to 6 respectively indicate the fixed base, sliding table, isolator under test, an external load, numerical computer, and power supply. It is worth noting that, in the experimental tests, the supply pressure P_s is less than the one used in simulations. It is worth noting that, the whole results have been plotted in the time interval 10s which only shows the dynamic process. However, the steady-state performances in the time interval $100s$ have already been verified, which has not been shown to improve the quality of the figures. According to the computer simulation results, the methods proposed AFFTESO, HG-ESO, HO-SMO, time-varying FT-ESO, and third-order FFTESO have had the best efficiency, respectively. However, since the HO-SMO is basically an approximate differentiator, measurement noise and unmodeled high-frequency dynamics put a practical limit on its use [32]. Besides, despite the straightforward design and the robustness against uncertainties and internal dynamics, the main limitation of the time-varying FT-ESO is the singularity problem, where the existed time-varying transformation grows unboundedly to infinity in real-world applications [29]. Therefore, without loss of generality, the performance of the presented AFFTESO has experimentally been evaluated along with HG-ESO and third-order FFTESO approaches that have already been confirmed as high-efficiency methods, where a large difference between the results is not expected. Figures 9-16 show that the state variables vary from zero initial conditions to the actual states in a finite time interval and rest around a small neighborhood of them. In this regard, although there is no large difference between the steady-state results, a clear difference in the transient performance is highlighted. For instance, according to Figures 9 and 10, the piston position and velocity varies from zero initial condition to the actual states in a finite time interval and rests around the small neighborhood of them. An estimation of the friction force is demonstrated in Figure 11. These experimental evaluations are consistent with the simulation results, which prove the performance of the proposed AFFTESO. This assessment on the real EHA system confirms that the proposed observer is practically efficient.

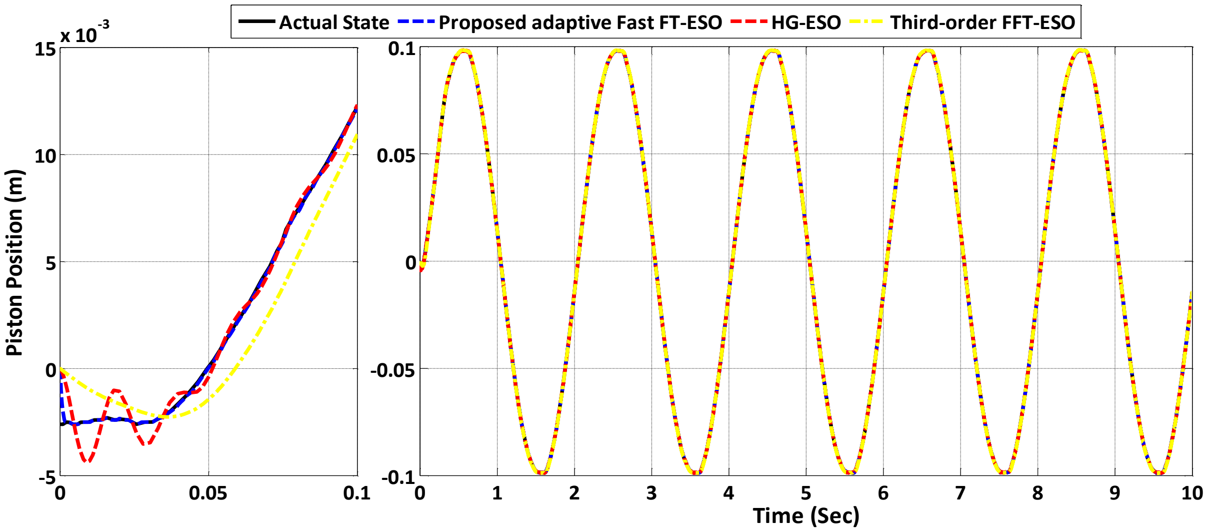

Figure 9. Real piston position and estimation results.

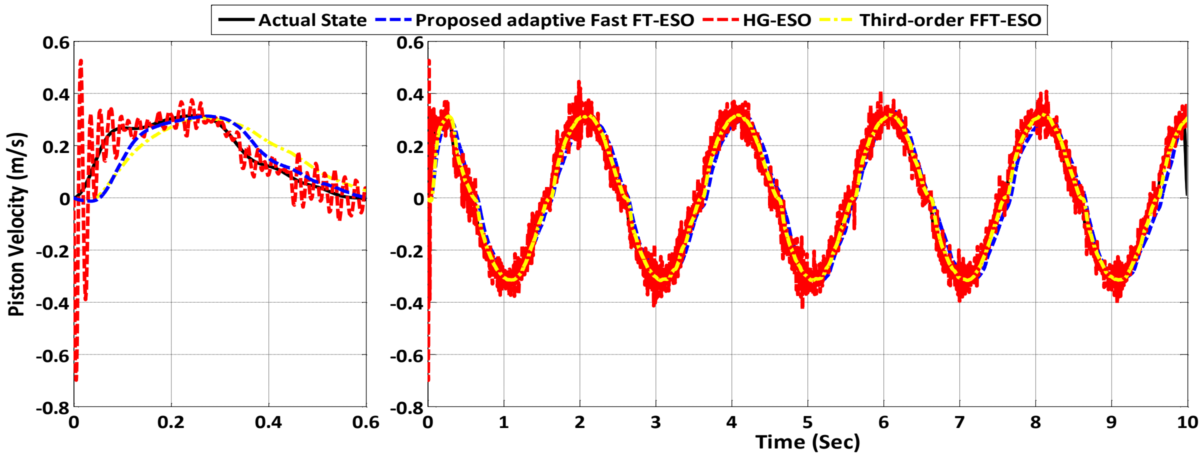

Figure 10. Real piston velocity and estimation results.

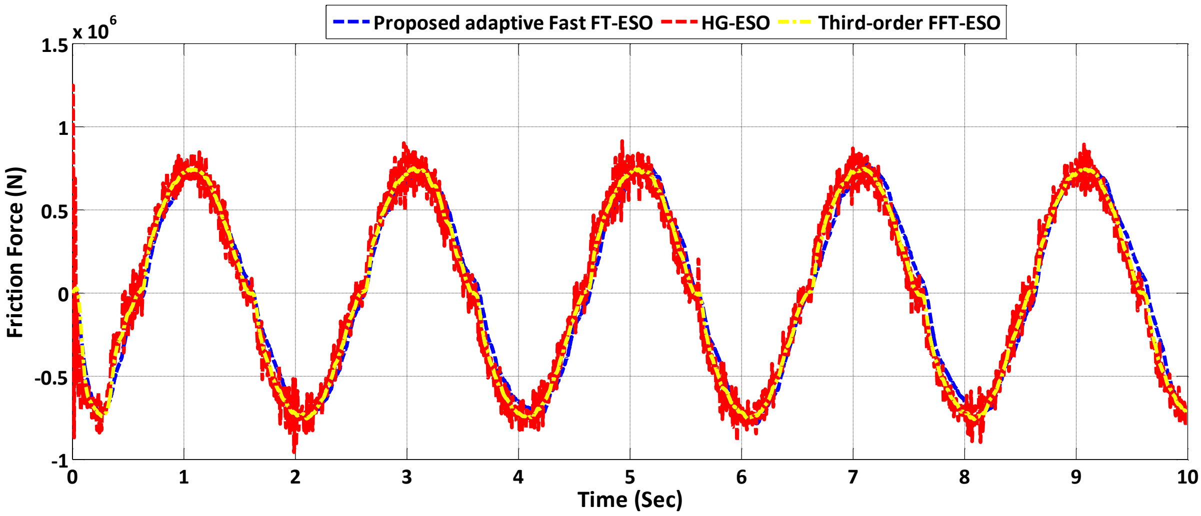

Figure 11. Estimation results of the friction force.

By using the defined RMS performance index J_1, the performance of all studied observers is evaluated in Table 3. The experimental results of the second-subsystem are shown in Figure 12 for the load pressure and Figure 13 for the dead-zone effects. It can be seen that by using the proposed AFFTESO, the estimated load pressure converges over a finite time to the actual pressure still maintaining the desired estimation of the dead-zone effects. By using the defined RMS performance index J_2, the performance of all studied observers is evaluated in Table 3, and it can be stated that one of the main challenges in real life systems, the robustness of observers against the state dependent uncertainties, is solved with satisfactory performance.

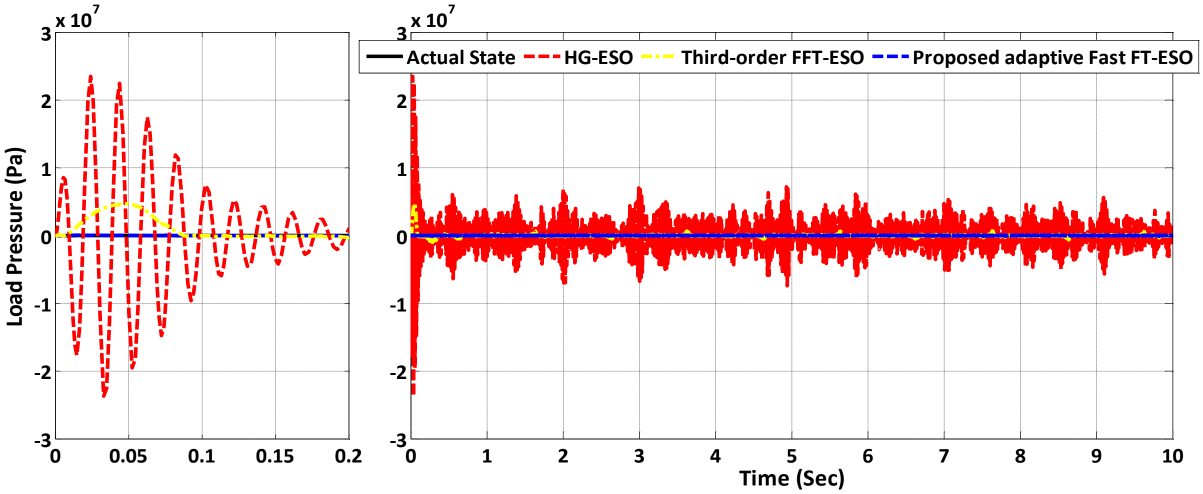

Figure 12. Real load pressure and estimation results.

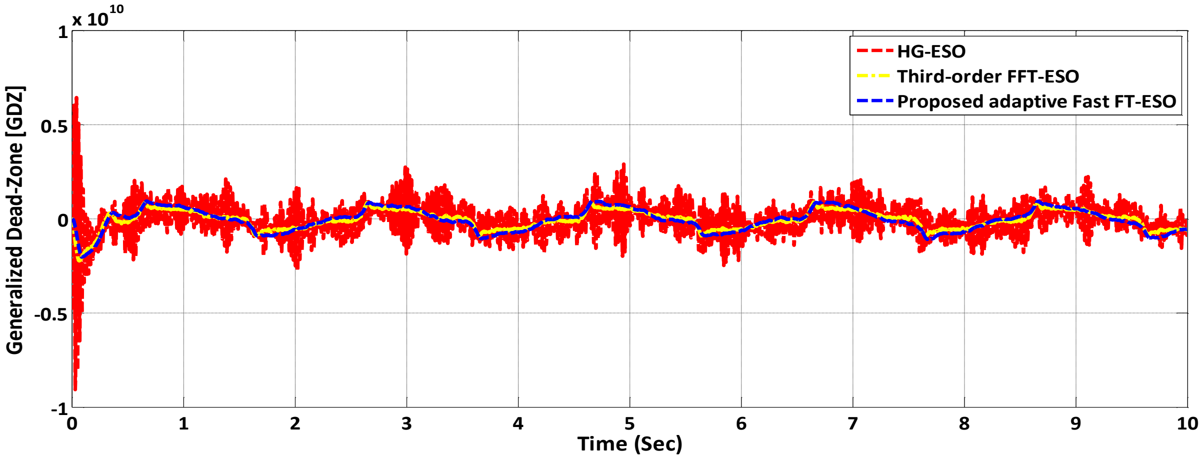

Figure 13. Estimation results of the dead-zone effects.

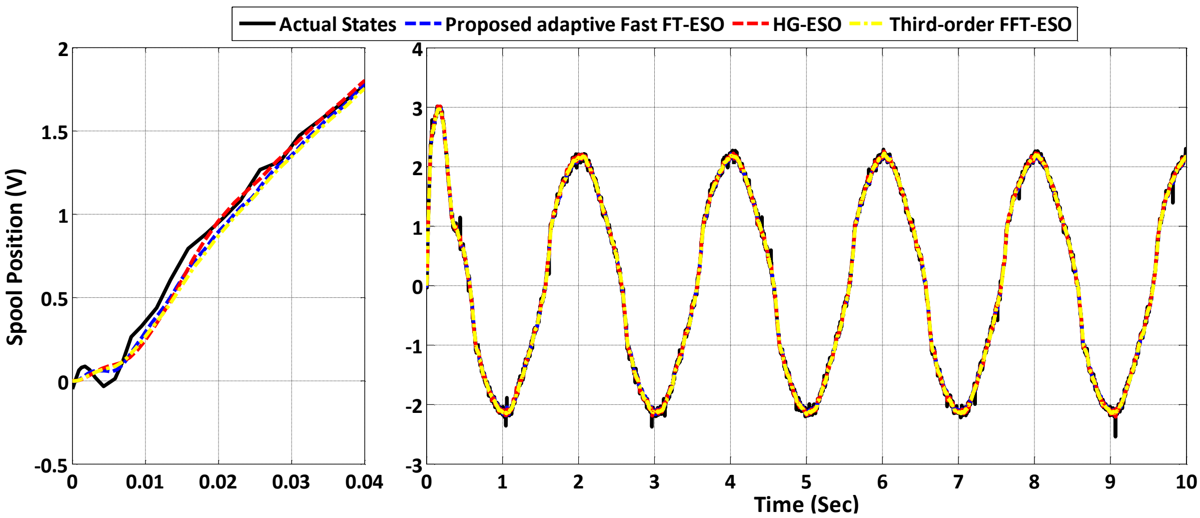

Figure 14. Real spool position and estimation results.

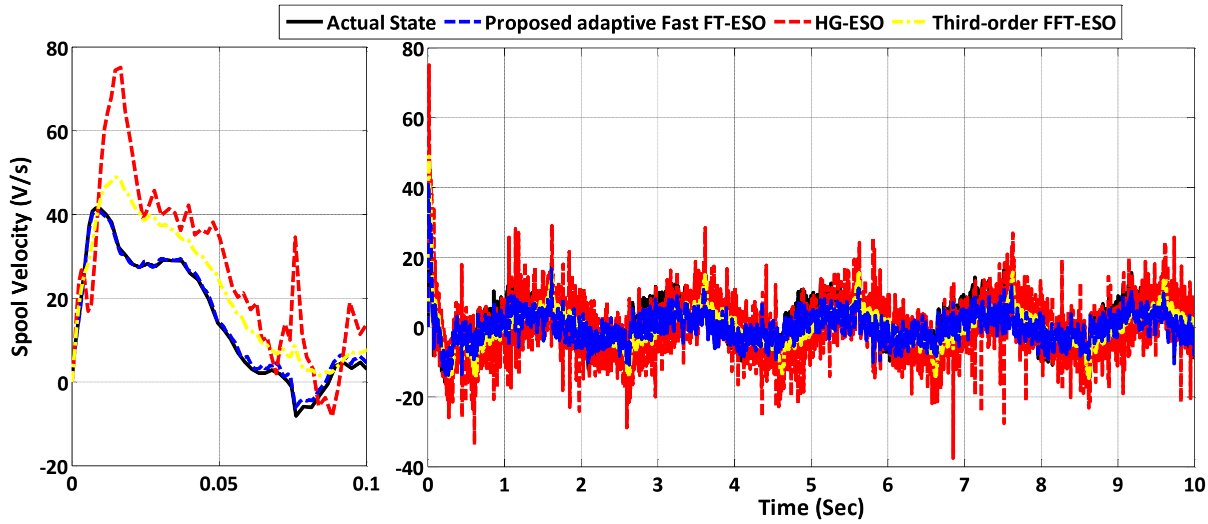

Figure 15. Real spool velocity and estimation results.

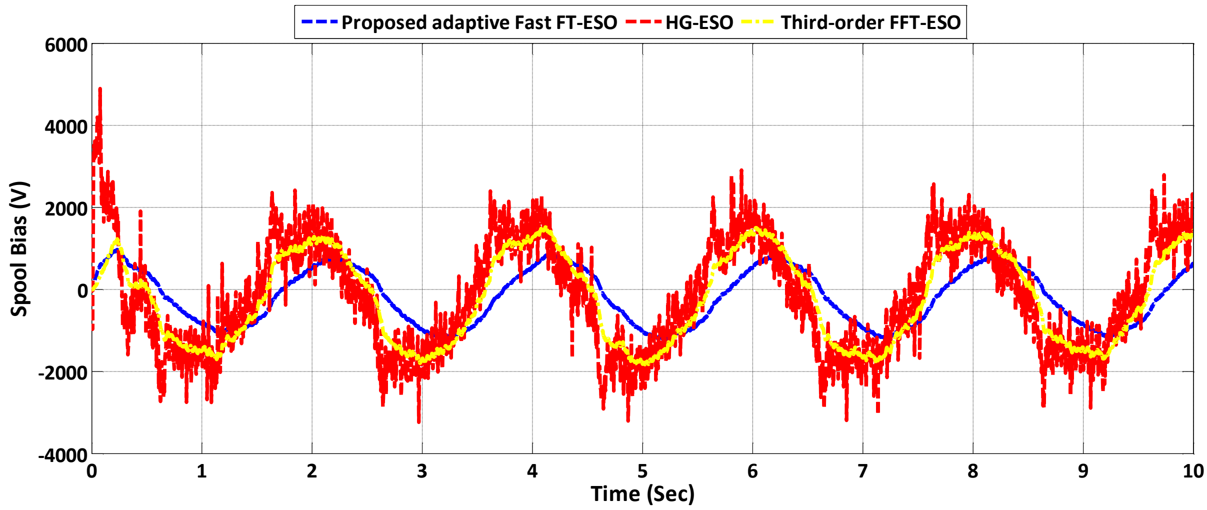

Figure 16. Estimation results of the spool bias.

According to Figures 14-16, it can be concluded that in comparison with the considered observers, the proposed AFFTESO provides finite-time estimation to state estimation with small errors as well as the acceptable finite-time estimation of the uncertainties. On the other hand, the HGESO, third-order FFTESO, and HO-SMO methods exhibit acceptable robust behaviors, but the experimental results reveal that the considered approaches experience large overshoot. By using the defined RMS performance index J_3 the performance of all studied observers is evaluated in Table 3, where the RMS performance index J_3 obtained using the proposed AFFTESO has the L_2 norm 2.08×10^5, where the HG-ESO and third-order FFTESO have the L_2 norm 5.79×10^5 and 4.09×10^5, respectively. Also, the RMS performance index J_1 obtained using the proposed AFFTESO has the L_2 norm 17.16×10^{-3}, where the HG-ESO and third-order FFTESO have the L_2 norm 58.84×10^{-3} and 19.02×10^{-3}, respectively. This numerical comparison confirms that the proposed strategy can be used to have acceptable estimations of the state variables regardless of the magnitude of the unknown terms.

Table 3

Comparative experimental results between the performance indexes.

	J_1 with physical unit $[m, {}^{m}/_{s}, N]^T$	J_2 with physical unit $\left[Pa, {}^{m^3}/_{s\,Pa^{\frac{1}{2}}}\right]^T$	J_3 with physical unit $[V, {}^{V}/_{s}, V]^T$
Proposed AFFTESO	$\begin{bmatrix} 12.53 \times 10^{-8} \\ 17.15 \times 10^{-3} \end{bmatrix}$	0.122×10^{16}	$\begin{bmatrix} 0.105 \\ 2.07 \end{bmatrix} \times 10^5$
HG-ESO [21]	$\begin{bmatrix} 26.26 \times 10^{-8} \\ 58.83 \times 10^{-3} \end{bmatrix}$	1.55×10^{16}	$\begin{bmatrix} 0.105 \\ 5.79 \end{bmatrix} \times 10^5$
Third-order FFTESO [20]	$\begin{bmatrix} 18.41 \times 10^{-8} \\ 19.01 \times 10^{-3} \end{bmatrix}$	0.557×10^{16}	$\begin{bmatrix} 0.105 \\ 4.08 \end{bmatrix} \times 10^5$

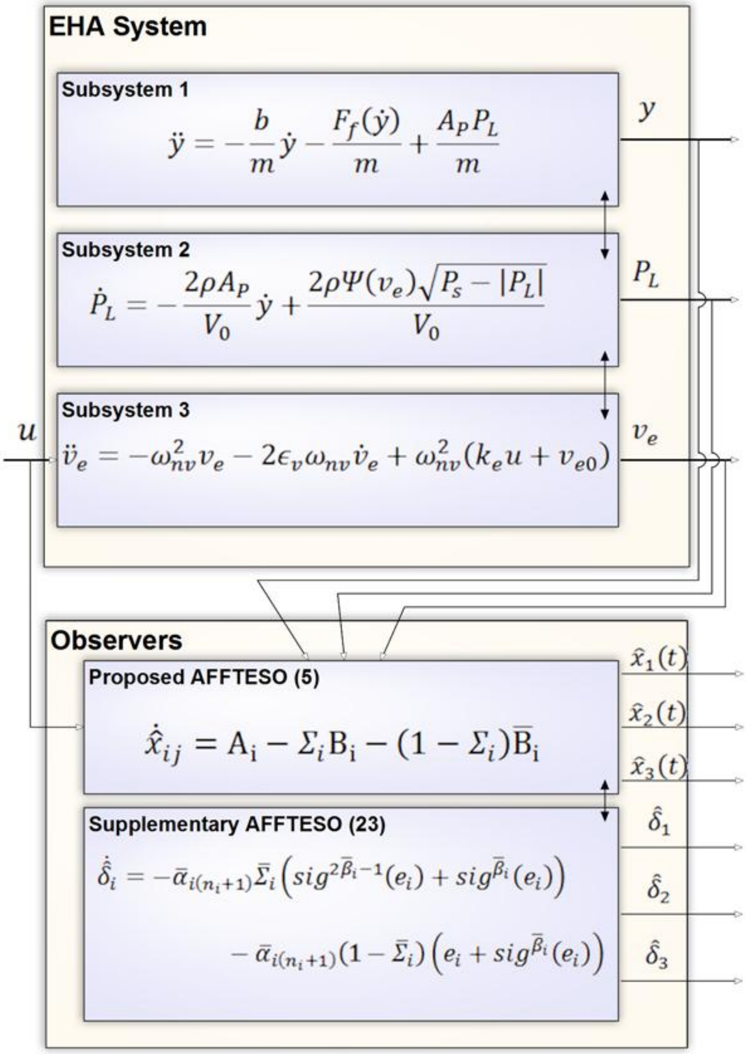

Figure 17. Block diagram of the proposed observers for the EHA system (1).

It can be concluded that the proposed strategy only requires measurements of the output variables y, P_L, and v_e, where without any knowledge about the upper bounds of the uncertainties, external disturbances, friction force, dead-zone effect, and spool bias, a negligible steady-state error is reached for the variables, which is quite acceptable from a control engineering perspective. Finally, it is worth noting that, although statistical issues such as maximum, minimum, mean, and standard deviation of estimation error have not been directly considered in this paper, by visually analyzing the results, it can be concluded that methods HG-ESO and third-order FFTESO have the most fluctuations, while the results of AFFTESO and HO-SMO show better efficiency. Besides, from the experimental results, it can be concluded that the proposed AFFTESO shows the lowest standard deviation of estimation error.

5. Conclusion

In this paper, the AFFTESO able to reconstruct the unmeasured state variables, external disturbances and uncertainties in a finite time is presented. This adaptive framework can be viewed as an extension of the fast finite-time observer canonical forms. In contrast to the earlier finite-time approaches, which only have a faster convergence rate around the equilibrium, the proposed AFFTESO solves this problem. The gains are changed based on the evaluation of the absolute value of the observation errors, where the convergence rate has an acceptable behavior both around the equilibrium points and far from them. In fact, the adaptive fast finite-time strategy forces the proposed observer to estimate the output measured variables of the EHA system in a finite time, where the desired estimations of the external disturbances, friction force, dead-zone effects, and spool bias are simultaneously guaranteed. Comparative simulations are presented to analyze the effectiveness of the proposed AFFTESO. The comparison between adaptive and fixed gains strategies shows that the proposed adaptive observer guarantees that the state estimation errors are uniformly bounded. Finally, the effectiveness of the proposed approach in real-life conditions is demonstrated through experimental studies. Although, the parameters of the considered observers have been adjusted in order to obtain the best possible observation results, the gain selection process does not follow an optimal procedure. Future activities will be devoted to present adaptive and optimal algorithms such as those proposed in [2, 33] for the selection of all the observer parameters. Besides, more theoretically, practically, and statistical analysis will be carried out in future works by adding noise to the EHA system to demonstrate the effectiveness of the proposed method in different loading scenarios on the actuator and changes in physical system parameters compared to other approaches.

Declaration of competing interest

The authors declare that they have no known competing financial interests or personal relationships that could have appeared to influence the work reported in this paper.

References

[1] C. Guan, S. Pan, S, Nonlinear adaptive robust control of single-rod electro-hydraulic actuator with unknown nonlinear parameters, IEEE Transactions on Control Systems Technology, 16(3) (2008) 434-445. https://doi.org/10.1109/TCST.2007.908195.

[2] V. Djordjevic, V. Stojanovic, H. Tao, X. Song, S. He, W. Gao, Data-driven control of hydraulic servo actuator based on adaptive dynamic programming, Discrete & Continuous Dynamical Systems-S, (2021). http://dx.doi.org/10.3934/dcdss.2021145.

[3] G. Palli, S. Strano, M. Terzo, A novel adaptive-gain technique for high-order sliding-mode observers with application to electro-hydraulic systems, Mechanical Systems and Signal Processing, 144 (2020) 106875. https://doi.org/10.1016/j.ymssp.2020.106875.

[4] P. Bernard, Observer design for nonlinear systems, Springer, 2019.

[5] H. Razmjooei, M.H. Shafiei, A novel finite-time disturbance observer-based partial control design: A guidance application, Journal of Vibration and Control, 26(11-12) (2020), 1001-1011. https://doi.org/10.1177%2F1077546319890951.

[6] H. Razmjooei, M.H. Shafiei, A new approach to design a finite-time extended state observer: Uncertain robotic manipulators application, International Journal of Robust and Nonlinear Control, 31(4) (2021) 1288-1302. https://doi.org/10.1002/rnc.5346.

[7] L. Zhang, C. Wei, R. Wu, N. Cui, Fixed-time extended state observer based non-singular fast terminal sliding mode control for a VTVL reusable launch vehicle, Aerospace Science and Technology, 82 (2018) 70-79. https://doi.org/10.1016/j.ast.2018.08.028.

[8] J. Davila, L. Fridman, A. Levant, Second-order sliding-mode observer for mechanical systems, IEEE transactions on automatic control, 50(11) (2005) 1785-1789. https://doi.org/10.1109/TAC.2005.858636.

[9] M. Dolgopolik, A.L. Fradkov, B. Andrievsky, Observer-based boundary control of the sine–Gordon model energy, Automatica, 113 (2020) 108682. [10] https://doi.org/10.1016/j.automatica.2019.108682.

[10] W. Xu, S. Qu, L. Zhao, H. Zhang, An improved adaptive sliding mode observer for middle-and high-speed rotor tracking, IEEE transactions on power electronics, 36(1) (2020) 1043-53. https://doi.org/10.1109/TPEL.2020.3000785.

[11] Y. Xiong, M. Saif, Sliding mode observer for nonlinear uncertain systems, IEEE transactions on automatic control, 46(12) (2011) 2012-2017. https://doi.org/10.1109/9.975511.

[12] G. Palli, S. Strano, M. Terzo, Sliding-mode observers for state and disturbance estimation in electro-hydraulic systems, Control Engineering Practice, 74 (2018) 58-70. https://doi.org/10.1016/j.conengprac.2018.02.007.

[13] B. Wang, Y. Shao, Y. Yu, Q. Dong, Z. Yun, DG. Xu, High-Order Terminal Sliding-Mode Observer for Chattering Suppression and Finite-Time Convergence in Sensor-less SPMSM Drives, IEEE Transactions on Power Electronics, 36(10) (2021) 11910-11920. https://doi.org/10.1109/TPEL.2021.3068495.

[14] J. Zhai, Z. Li, Fast-Exponential Sliding Mode Control of Robotic Manipulator with Super-Twisting Method, IEEE Transactions on Circuits and Systems II: Express Briefs, 1 (2021). https://doi.org/10.1109/TCSII.2021.3081147.

[15] O. Barambones, JA. Cortajarena, I. Calvo, JM. De-Durana, P. Alkorta, A. Karami-Mollaee, Real time observer and control scheme for a Wind Turbine System based on a high order sliding modes, Journal of the Franklin Institute, 358(11) (2021) 5795-5819. https://doi.org/10.1016/j.jfranklin.2021.05.022.

[16] V. Andrieu, L. Praly, A. Astolfi, Homogeneous approximation, recursive observer design, and output feedback, SIAM Journal on Control and Optimization, 47(4) (2008) 1814-1850. https://doi.org/10.1137/060675861.

[17] F. Lopez-Ramirez, A. Polyakov, D. Efimov, W. Perruquetti, Finite-time and fixed-time observer design: Implicit Lyapunov function approach, Automatica, 87 (2018) 52-60. https://doi.org/10.1016/j.automatica.2017.09.007.

[18] M.V. Basin, P. Yu, Y.B. Shtessel, Hypersonic missile adaptive sliding mode control using finite-and fixed-time observers, IEEE Transactions on Industrial Electronics, 65(1) (2017) 930-941. https://doi.org/10.1109/TIE.2017.2701776.

[19] T. Ménard, E. Moulay, W. Perruquetti, Fixed-time observer with simple gains for uncertain systems, Automatica 81 (2017) 438-446. https://doi.org/10.1016/j.automatica.2017.04.009.

[20] N. Ali, I. Tawiah, W. Zhang, Finite-time extended state observer based nonsingular fast terminal sliding mode control of autonomous underwater vehicles, Ocean Engineering, 218 (2020) 108179. https://doi.org/10.1016/j.oceaneng.2020.108179.

[21] D. Won, W. Kim, M. Tomizuka, Nonlinear Control With High-Gain Extended State Observer for Position Tracking of Electro-Hydraulic Systems, IEEE/ASME Transactions on mechatronics, 25(6) (2020) 2610-2621. https://doi.org/10.1109/TMECH.2020.2985619.

[22] J. Lee, J. Seo, J. Choi, Output feedback control design using Extended High-Gain Observers and dynamic inversion with projection for a small scaled helicopter, Automatica, 133 (2021). https://doi.org/10.1016/j.automatica.2021.109883.

[23] D. Chowdhury, H.K. Khalil, Dynamic consensus and extended high gain observers as a tool to achieve practical frequency synchronization in power systems under unknown time-varying power demand, Automatica, 131 (2021) 109753. https://doi.org/10.1016/j.automatica.2021.109753.

[24] L. Wang, Z. Gao, X. Zhou, Z. Han, Exponential stabilization of a star-shaped thermo-elastic network system based on the extended state observer with time-varying gains, IEEE Transactions on Automatic Control, 66(1) (2020) 267-274. https://doi.org/10.1109/TAC.2020.2976317.

[25] H. Razmjooei, M.H. Shafiei, G. Palli, M.M. Arefi, Non-linear finite-time tracking control of uncertain robotic manipulators using time-varying disturbance observer-based sliding

mode method, Journal of Intelligent & Robotic Systems, 104(2) (2022) 1-13. https://doi.org/10.1007/s10846-022-01571-x.

[26] S. Djennoune, M. Bettayeb, U.M. Al-Saggaf, Modulating function-based fast convergent observer and output feedback control for a class of non-linear systems, IET Control Theory & Applications, 13(16) (2019) 2681-2693. https://doi.org/10.1049/iet-cta.2018.5313.

[27] J. Holloway, M. Krstic, Prescribed-time output feedback for linear systems in controllable canonical form, Automatica, 107 (2019). https://doi.org/10.1016/j.automatica.2019.05.027.

[28] H. Razmjooei, M.H. Shafiei, E. Abdi, A Novel Continuous Finite-Time Extended State Observer Design for a Class of Uncertain Nonlinear Systems, IEEE Access. (2020). https://doi.org/10.1109/ACCESS.2020.3043725.

[29] H. Razmjooei, M.H. Shafiei, G. Palli, A. Ibeas, Chattering-free robust finite-time output feedback control scheme for a class of uncertain non-linear systems, IET Control Theory & Applications, 14(19) (2020) 3168-3178. https://doi.org/10.1049/iet-cta.2020.0910.

[30] P.J. Antsaklis, A.N. Michel, Linear systems (Vol. 8), New York: McGraw-Hill, 1997.

[31] Q. Hu, B. Jiang, Continuous finite-time attitude control for rigid spacecraft based on angular velocity observer, IEEE Transactions on Aerospace and Electronic Systems, 54(3) (2017) 1082-1092. https://doi.org/10.1109/TAES.2017.2773340.

[32] H.K. Khalil, J.W. Grizzle, Nonlinear systems, Upper Saddle River, NJ: Prentice hall, 2002.

[33] H. Fang, G. Zhu, V. Stojanovic, R. Nie, S. He, X. Luan, F. Liu, Adaptive optimization algorithm for nonlinear Markov jump systems with partial unknown dynamics, International Journal of Robust and Nonlinear Control, 31(6) (2021) 2126-2140. https://doi.org/10.1002/rnc.5350.